Reports of the Department of Geodetic Science and Surveying
Report No. 336

THE INDIRECT EFFECTS ON THE COMPUTATION OF GEOID UNDULATIONS

by
Chugiat Wichiencharoen

Prepared for

National Aeronautics and Space Administration
Goddard Space Flight Center
Greenbelt, Maryland 20770

NASA Grant No. NGR 36-008-161
OSURF Project 783210

The Ohio State University
Department of Geodetic Science and Surveying
1958 Neil Avenue
Columbus, Ohio 43210

December, 1982

Reports of the Department of Geodetic Science and Surveying

Report No. 336

THE INDIRECT EFFECTS ON THE COMPUTATION OF GEOID UNDULATIONS

by

Chugiat Wichiencharoen

Prepared for

National Aeronautics and Space Administration
Goddard Space Flight Center
Greenbelt, Maryland 20770

NASA Grant No. NGS 36-008-161
OSURF Project 783210

The Ohio State University
Department of Geodetic Science and Surveying
1958 Neil Avenue
Columbus, Ohio

December, 1982

ABSTRACT

The indirect effects on the geoid computation due to the second method of Helmert's condensation were studied. When Helmert's anomalies are used in Stokes' equation, there are three types of corrections to the free-air geoid. The first correction, the indirect effect on geoid undulation due to the potential change in Helmert's reduction, had a maximum value of 0.51 meters in the test area covering the United States. The second correction, the attraction change effect on geoid undulation, had a maximum value of 9.50 meters when the 10° cap was used in Stokes' equation. The last correction, the secondary indirect effect on geoid undulation, was found negligible in the test area. The corrections were applied to uncorrected free-air geoid undulations at 65 Doppler stations in the test area and compared with the Doppler undulations. Based on the assumption that the Doppler coordinate system has a z-shift of 4 meters with respect to the geocenter, these comparisons showed that the corrections presented in this study yielded improved values of gravimetric undulations.

Foreward

This report was prepared by Mr. Chugiat Wichiencharoen, Graduate Research Associate, the Department of Geodetic Science and Surveying, The Ohio State University under NASA Grant NGR36-008-161, The Ohio State University Research Foundation Project No. 783210. The grant covering this research is administered through the NASA Goddard Space Flight Center, Greenbelt Maryland, 20771, Mr. Jean Welker, Technical Officer.

A modified version of this report was submitted to the Graduate School of the Ohio State University in partial fulfillment of the requirements for the degree Master of Science.

Acknowledgments

I am very grateful to Dr. Richard H. Rapp for his guidance and support throughout the course of this research project. I wish to thank Dr. Dhaneshwar P. Hajela for his valuable comments and suggestions. The discussion with Dr. Helmut Moritz is appreciated. Thanks also go to my wife, Tasnee Wichiencharoen, who typed the report drafts and to Susan Carroll and Laura Brumfield for their typing of this report.

The computer funds were provided by the Instruction and Research Computer Center at the Ohio State University, through the Department of Geodetic Science and Surveying.

TABLE OF CONTENTS

List of Notations

N	geoid undulation
Δg	gravity anomaly
h	height above the geoid
R	mean radius of the earth
γ	normal gravity at the point on the reference ellipsoid
$S(\psi)$	Stokes' function
$d\sigma$	element of solid angle
W,V	gravity potential and gravitational potential, respectively
$\delta W,\delta V$	gravity and gravitational potential change, respectively
δN	indirect effect due to the potential change
ΔN	attraction change effect on geoid undulation
δ	secondary indirect effect on gravity
$A,\delta A$	vertical attraction and attraction change, respectively
C	terrain correction
k	Newton's gravitational constant
ρ	volume density
κ	surface density
ψ	angular radius from the evaluation point
a	linear radius from the evaluation point
$( )'$	quantity referred to the regular part of topography
$( )''$	quantity referred to the irregular part of topography
$( )_T$	quantity referred to the topography before the condensation
$( )_C$ or $( )_s$	quantity referred to the condensed layer, i.e., after the condensation
P	point on the earth's surface (see figure 1)
P_o	point on the geoid (see figure 1)
Q_o	point on the reference ellipsoid corresponding to point P_o (see figure 1)
$\bar{C}_{nm},\bar{S}_{nm}$	fully normalized geopotential coefficients
SBP	spherical Bouguer plate (figure 4, p. 22)
PCP	plane circular plate (figure 5, p. 23)
TDSBP	Two Difference Spherical Bouguer Plate (p. 35)
TDPCP	Two Difference Plane Circular Plate (p. 35)

1. Introduction

A fundamental equation used to compute geoid undulation, N is the Stokes' integral equation;

$$N = \frac{R}{4\pi\gamma} \iint_{\sigma} \Delta g \, S(\psi) \, d\sigma \qquad (1)$$

Equation (1) is valid for a reference ellipsoid which (i) has the same potential as the geoid, (ii) encloses a mass that is numerically equal to the earth's mass, and (iii) has its center at the center of mass of the earth (Heiskanen and Moritz, 1967, p. 94). This implies that the gravity anomaly, Δg used in equation (1) refers to the geoid with no external masses. This important assumption necessitates the real earth to be regularized so that all masses outside the geoid are completely removed or shifted below the geoid. The process of removing or shifting the masses is called a gravity reduction.

To properly obtain the gravity anomaly on the geoid, we must consider the effect of removing or shifting the masses outside the geoid on the value of gravity g_{obs} at point P on the earth's surface. Then, after removing or shifting the masses, the gravity station is brought down along the vertical curve to point P_o on the geoid (see Figure 1). In other words, the gravity force is transferred from point P to point P_o by a free air reduction. By subtracting the normal gravity γ at the corresponding point, Q_o, on the ellipsoid from the gravity at P_o we then obtain the gravity anomaly on the geoid.

By removing or shifting the masses outside the geoid in the gravity reduction process the original potential of the earth is changed as well. Suppose that the geoid is defined to be the equipotential surface having potential W_o and the reduction process causes the change in potential at a point originally on the geoid by the amount of δW. To be precise, δW is defined to be the gravity potential of the actual topographic masses minus the gravity potential of the masses after the reduction process. This means that the point originally on the geoid now has the potential $W_o - \delta W$ (the negative

sign is conventional, see below) and by definition it is not the point on the geoid anymore. We call the changed geoid as the cogeoid. Hence the surface computed by Stokes' equation using the gravity anomaly reduced by the explained process so far is not the geoid but the cogeoid. The real geoid and the cogeoid are separated by a vertical distance δN which is called an indirect effect of gravity reduction on geoid undulation. δN is simply computed by Brun's formula:

$$\delta N = \frac{\delta W}{\gamma} \tag{2}$$

where δW is the gravity potential change at the geoid and γ is the normal gravity on the ellipsoid. A positive δN means that the geoid is above the cogeoid.

The potential of gravity, W is the sum of the potentials of gravitational force, V and centrifugal force, Φ, i.e., $W = V + \Phi$. Now we are interested in the change of gravity potential, δW or the difference between the gravity potentials of the masses before and after the gravity reduction. Since the potentials of the centrifugal forces of the masses before and after the gravity reduction are the same, the change of gravity potnetial, δW is then the same as the change of gravitational potential, δV. Brun's formula in equation (2) becomes:

$$\delta N = \frac{\delta V}{\gamma} \tag{3}$$

Therefore, the potential change can be referred to as either the change in gravity potential or the change in gravitational potential.

Secondary Indirect Effect on Gravity

Since Stokes' equation gives the surface of the cogeoid rather than the geoid then to be more accurate, the gravity anomaly used in the equation must be the boundary value on the computed surface, i.e., the gravity station is further brought down from point P_0 on the geoid to point

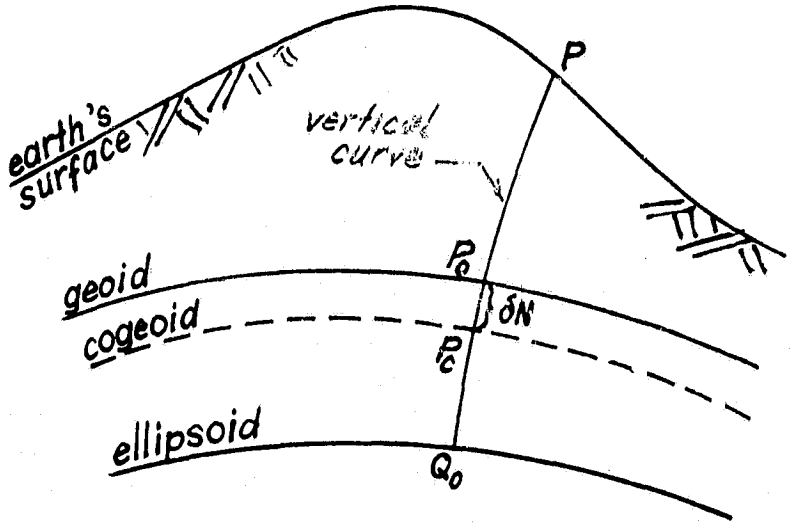

Figure 1: Geoid, cogeoid and ellipsoid

P_c on the cogeoid (see Figure 1) before Stokes' equation can be applied. In order to bring the gravity station from the geoid to the cogeoid, it is done by a simple "free-air reduction" (Heiskanen and Mortiz, 1967, p. 142). The condensation reduction is unnecessary because the masses between the geoid and cogeoid are relatively small compared to the masses above the geoid. The movement of such small mass through the very small distance will produce no significant change in δW . Therefore, it can be thought that instead of moving the masses inside the geoid in the first place, we immediately put them inside the cogeoid with δW remaining unchanged (Bomford, 1971, p. 493).

The change of gravity by free-air reduction in bringing down the point for the vertical distance h is computed by

$$F = - \frac{\partial g}{\partial h} \cdot h$$

In practice, the vertical gradient of gravity $\partial g/\partial h$, is replaced by the normal gradient $\partial\gamma/\partial h$ so we have

$$F = -\frac{\partial\gamma}{\partial h} \cdot h$$
$$= +0.3086h \qquad \text{mgal} \tag{4}$$

for h in meters. From the above equation, the change in gravity in bringing down the gravity station from point P_o on the geoid to point P_c on the cogeoid can be computed from:

$$\delta = 0.3086 \ \delta N \qquad \text{mgal} \tag{5}$$

where δN is the separation between the geoid and cogeoid or the indirect effect on geoid undulation in meters. The effect of δ is called "a secondary indirect effect on gravity" (Heiskanen and Moritz, 1967, p. 142.)

Considering these two indirect effects caused by the gravity reduction, the undulation of the geoid, N is

$$N = \frac{R}{4\pi\gamma} \iint_{\sigma} (\Delta g + \delta) \ S(\psi) \ d\sigma + \delta N \tag{6}$$

where Δg is the gravity anomaly at point P_o on the geoid.

Gravity Reduction

There are several ways in which the gravity reduction can be performed. Individual methods differ, depending on how the topographic masses above the geoid are treated. For example, the Bouguer reduction completely removes the topographic masses. The free-air reduction, in concept, ignores the existence of the masses so the gravity on the topographic surface is reduced to the geoid using the vertical component of the gravity gradient. The second method of Helmert's condensation shifts and condenses the topographic masses on the layer of the geoid

while an isostatic reduction distributes the masses to a certain depth under the geoid. More methods and more details can be found in standard textbooks in physical geodesy, e.g. Heiskanen and Moritz (1967), Bomford (1971), and Grushinsky (1969).

Theoretically, all gravity reductions are equivalent and lead to the same geoid provided that they are properly applied, i.e., the indirect effect is taking into consideration (Heiskanen and Moritz, 1967). In practice, however, gravity reductions which give a large indirect effect are avoided in determining the geoid. Usually, a free-air anomaly at sea level is used in Stokes' equation and is said to be an approximation of Helmert's gravity anomaly (Heiskanen and Moritz, 1967, p. 146). The indirect effect due to Helmert's reduction is less than 50 cm for the topograhic height of 3 km (Heiskanen and Moritz, 1967, p. 145; Grushinsky, 1969, and Neequaye, 1975); therefore, it may not necessarily be considered. However, the required accuracy of geoid undulations may be on the order of 10 cm or less in the future. This means that the indirect effects cannot be neglected anymore.

Since the free-air anomaly is mostly used in practice and closely related to the anomaly of the second method of Helmert's condensation. It is interesting for us to look into more details of these two anomalies.

Free Air Anomaly vs. Helmert's Anomaly

Helmert introduced two methods of condensation. In the first method, the topography is condensed on a parallel surface located 21 kilometers below the geoid (Heiskanen and Moritz, 1967, p. 145). The value of 21 kilometers, the difference between the semimajor and semiminor axes of the earth, is adopted in order to avoid problems connected with the convergence of the spherical harmonic series for the potential outside the earth. The first method is not popular and not used by geodesists. The second method of Helmert's condensation is therefore the one which is referred to in most literature and also in this study.

In the second method of Helmert's condensation, the topographic masses of volume density ρ above the geoid are shifted and condensed to be a surface layer of surface density ρh, where h is the height of the topographic surface above the geoid. After condensation, the gravity force at point P on the earth's surface is transferred to the corresponding point, P_0, on the geoid using the vertical gradient of gravity. In a free-air reduction, the gravity force is just transferred from point P on the surface to point P_0 on the geoid by the vertical gradient of gravity, without doing anything with the topographic masses. This means that if gravity g_{obs} is measured at point P on the topogrpahic surface, the gravity at point P_0 on the geoid becomes $g_{obs} + F$ where F is the change in gravity by the free-air reduction computed by equation (4). After subtracting normal gravity, γ, at the corresponding point on the ellipsoid, we get a free-air anomaly on the geoid as:

$$\Delta g = g_{obs} + F - \gamma \tag{7}$$

A gravity anomaly of the geoid obtained by the second method of Helmert's condensation, shortly called here as Helmert's gravity anomaly, Δg_H, differs from the free-air anomaly at the same point by the amount of terrain correction C (Lambert, 1930, p. 116), that is,

$$\Delta g_H = \Delta g + C \tag{8}$$

Equation (8) is obtained based on the linear approximations for the effect of topography (Moritz, 1968). We will see later that C is only one part of the total attraction change due to the second method of Helmert's condensation.

Considering the procedure in the second method of Helmert's condensation, we see that this method maintains the same earth's mass and the same location of the center of the mass of the earth (Bomford, 1971, p. 505). That is the second method of Helmert's condensation fulfills the second and the third requirements of Stokes' equation. The first requirement is

always fulfilled by keeping the definition of the geoid which is the equipotential surface having potential W_0. Realizing these facts, we see that using the gravity anomalies obtained from the second method of Helmert's condensation in equation (6) should give the more correct geoid undulations than using the ones from the free-air reduction. By using the gravity anomaly of equation (8) in equation (6), the more accurate geoid undulation becomes

$$N = \frac{R}{4\pi\gamma} \iint_{\sigma} (\Delta g + C + \delta)\, S(\psi)\, d\sigma + \delta N \tag{9}$$

$$= \frac{R}{4\pi\gamma} \iint_{\sigma} \Delta g\, S(\psi)\, d\sigma + \frac{R}{4\pi\gamma} \iint_{\sigma} C\, S(\psi)\, d\sigma + \frac{R}{4\pi\gamma} \iint_{\sigma} \delta S(\psi)\, d\sigma + \delta N \tag{10}$$

$$N = N_1 + \Delta N_1 + \delta N_2 + \delta N \tag{11}$$

We see that N_1 is the undulation which has normally been computed from free-air anomalies and used as the 'correct' undulation. This means that if the free-air anomalies, Δg are used in Stokes' equation (1), there are three kinds of errors incurred in determining the geoid. One comes from neglecting the terrain effect in the gravity reduction and the other two from the indirect effects. In sequel, we will refer correction ΔN_1 which comes from the attraction change in Helmert's condensation method as an attraction change effect on geoid undualtion; correction δN which comes from the potential change as an "indirect effect" and correction δN_2 as a "secondary indirect effect".

In the following sections, we will investigate how large each correction is.

2. Investigation of Formulas for Computation

It is shown in the previous chapter (equation (11)) that the accurate geoid undulation can be computed by: (i) using the gravity anomalies obtained from the second method of Helmert's condensation in Stokes' equation and (ii) taking the indirect effects on geoid undulation and on gravity into consideration. In other words, if free-air anomalies instead of Helmert's anomalies are used in Stokes' equation, we must compute the corrections caused by the potential change and the attraction change in the process of Helmert's condensation reduction (the second method). In literature, various models of topographic masses are used to derive or to estimate the effects of potential change and attraction change in the reduction process, for example: a spherical Bouguer plate (i.e., a portion of a spherical shell); a plane circular plate (i.e., a plane plate with finite radius); and a plane Bouguer plate (i.e., an infinite plane plate). These examples of topograpgic models are referred to as "the regular part" or "the smooth part" of the topography because the irregularity of the topography is not taken into consideration in these models. When the irregularity of the topography is considered in the model, the masses above and the non-existing masses below the upper surface of the regular part of the topography are referred to as the irregular part of the topography.

In this chapter we investigate the existing expressions to see which type of model and which expressions we should use to get the geoid computation of 10 centimeter accuracy. Before we pick up the appropriate expressions for investigation, there is a little confusion to be made clear. The confusion concerns the location of the computation point where we compute the changes in gravity potential and gravity attraction due to the reduction process. The following is a literature review that involves the computation point for the potential change and the attraction change in the second method of Helmert's condensation.

In the derivation of Moritz (1968), he derives the gravitational potential of the topographi masses, V, at a point P on the earth's surface. The potential of the condensed layers, V_s, is implied to be lying on point P_o at sea level (Ibid., p. 18). The attraction of the topographic masses and the condensed layer, A and A_s respectively are both referred to the same point P. By linear approximations for the topographic effect, Moritz shows that $V = V_s$ and $A = A_s - C$ where C is the quantity known as a terrain correction (Ibid., eq. (67)).

The change in gravity due to the condensation of topography to sea level by Bomford (1971) is evaluated at point P on the earth's surface This gravity change is zero if the topography is assumed to be a spherical shell or an infinite plane as Bomford states that "Condensing the plateau to below the geoid causes no change in g, whether the plateau is regarded as an infinite plane or as a spherical shell." There is no definite statement, however, concerning the point where the change in potential due to the condensation method is evaluated.

Neequaye (1975) uses a plane circular plate with finite radius a thickness b and volume density ρ as a topographic model (see figure 2). He obtains a general expression for computing the gravitational potential of the topographic masses at some point of height c directly above the center of the bottom surface of the circular plate as (Ibid., eq. (3-1)):

$$V = \pi k\rho[(c-b)^2 - c^2 - (c-b)\sqrt{a^2+(c-b)^2} + c\sqrt{a^2+c^2}$$

$$-a^2 \ell n(c-b+\sqrt{a^2+(c-b)^2}) + a^2 \ell n(c+\sqrt{a^2+c^2})] \qquad (12)$$

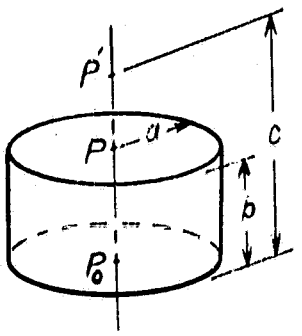

Figure 2: A topographic model used by Neequaye (1975)

The potential change is the difference between the potential of the actual topographic mass and the potential of the condensed layer. To get the potential of the topographic mass, V_T, the distance c is set equal to b. Equation (12) becomes:

$$V_T = \pi k\rho \left(-b^2+b\sqrt{a^2+b^2} + a^2 \ell n \frac{b+\sqrt{a^2+b^2}}{a}\right) \qquad (13)$$

This means that the potential of the topography is evaluated at point P on the earth's surface.

To get the potential of the condensed layer, the quantity ρ in the equation (12) is set to $\frac{\kappa}{b}$. By taking the limit $b \to 0$, equation (12) becomes

$$V_c = 2\pi k\rho b \ (\sqrt{a^2 + c^2} - c).$$

Then by setting c equal to b, we get

$$V_c = 2\pi k\rho b \ (\sqrt{a^2 + b^2} - b) \tag{14}$$

The potential of the condensed layer is again evaluated at the point P. Therefore, the potential change:

$$\delta V = V_T - V_c$$

$$= \pi k\rho\{b^2 - b\sqrt{a^2 + b^2} + a^2 \ell n \frac{b + \sqrt{a^2 + b^2}}{a}\} \tag{15}$$

is evaluated at the point P on the earth's surface.

Grushinsky (1969) uses a plane circular plate with an infinite radius for computing the potential change. His derivation implies that the potential due to topography refers to point P on the earth's surface while the potential due to the condensed layer refers to point P_o on the geoid. However, because of the symmetry of a plane circular plate, the gravitational potential due to the topography at point P on the surface and at point P_o on the geoid are exactly the same. Therefore, the approximate formula for potential change that has been obtained can be referred to a point P_o on the geoid.

Lambert (1930, p. 116) makes a clear statement in regard to finding the reduced gravity at point P_o on the geoid. Apart from the free-air reduction, we must apply a correction to the measured gravity at P on the earth surface. This correction is equal to the attraction of the condensed topography at P_o on the geoid minus the attraction of the topography at P on the earth's surface. When Lambert derives the potentials in isostatic reduction, the compuation points he refers

to are the same as those to which he refers for the attractions (Ibid., p. 150). Helmert's condensation reduction can be viewed as a special case of isostatic reduction where the compensation depth is zero (Heiskanen and Moritz, 1967, p. 145 and Bomford, 1971, p. 497). This means that the gravitational potential of the topography refers to the point P on the earth's surface and the potential of the condensed layer refers to the point P_o on the geoid.

Baeschlin (1948, Chapter XII) uses the point P as the computation point for the attraction difference between the actual topography and the compensated topography in the isostatic reduction method. He uses the point P_o on the geoid as the computation point for potential change.

Heiskanen and Moritz (1967, Chapter 3) refer the computation point to point P on the surface when the attractions of the topography and the condensed layer are determined in Helmert's condensation reduction. They also point out that to compute the potentials of the topography and the condensed layer, the point to which the potentials refer is always the point P_o on the geoid.

From the above literature review, we see some confusion in using computation points for the potential change and the attraction change in the second method of Helmert's condensation between point P on the earth's surface and point P_o on the geoid. To understand what would be the reason which causes the confusion, we take a spherical shell to represent the topography of the earth. Let the thickness of the shell, h_p represent the height of the topography and M_s be the masses of the spherical shell with constant volume density ρ. The mass M_s can be computed from:

$$M_s = \rho \times \text{volume of the spherical shell}$$

$$= \rho \cdot \tfrac{4}{3}\pi[(R + h_p)^3 - R^3]$$

$$= \frac{4\pi\rho}{3}\ (3R^2 h_p + 3Rh_p^2 + h_p^3) \qquad (16)$$

Introduce $u = h_p/R$, then

$$M_s = 4\pi\rho R^2 h_p \left(1 + u + \tfrac{1}{3}u^2\right) \tag{17}$$

When evaluation point at P on the earth's surface.

To evaluate the potential of the spherical shell at point P on the earth's surface, the whole masses of the shell are acting like a point mass at the center of the shell because of the symmetry of the shell. That is the gravitational potential of the shell at point P symbolized by $V'|_P$ can be written as:

$$V'|_P = \frac{kM_s}{(R+h_P)} = \frac{kM_s}{R(1+u)} \tag{18}$$

Expanding $(1+u)^{-1} = 1-u+u^2-u^3+ \ldots$ and substituting for M_s, we have

$$V'|_P = k\cdot 4\pi\rho R h_P \left(1+u+\tfrac{1}{3}u^2\right)\left(1-u+u^2-u^3+ \ldots\right)$$

$$= 4\pi k\rho R h_p\left(1+\tfrac{1}{3}u^2 - \tfrac{1}{3}u^3+ \ldots\right) \tag{19}$$

To get the vertical attraction of the spherical shell at point P on the earth's surface, we have

$$A'|_P = -\frac{\partial}{\partial R} V'|_P \tag{20}$$

$$= -\frac{kM_s}{(R+h_p)^2}$$

$$= \frac{-kM_s}{R^2(1+u)^2} \tag{21}$$

since $(1+u)^{-2} = 1-2u+3u^2-4u^3+ \ldots$, then we get

$$A'|_P = -4\pi k\rho h_p \left(1-u+\tfrac{4}{3}u^2-\tfrac{5}{3}u^3+ \ldots\right) \tag{22}$$

When the spherical shell is condensed to be a layer surface on the geoid, this layer has the same mass M_s and can still be considered as the point mass at the center of the sphere, i.e., the potential of the condensed layer, V'_s at point P on the earth surface is:

$$V'_{s|P} = \frac{kM_s}{(R+h_p)} = V'_{|P} \tag{23}$$

The vertical attraction of the condensed layer at point P, $A'_{s|P}$ is also equal to $A'_{|P}$.

When evaluation point at P_o on the geoid.

To evaluate the potential of the spherical shell at point P_o on the geoid, we cannot consider the shell as a point mass anymore since the evaluating point is now inside the shell. For a point inside the shell at a distance r from the center, the potential of the shell is (MacMillan, 1958, p. 38):

$$V' = 4\pi k\rho \left[\tfrac{1}{2}(R+h_p)^2 - \tfrac{1}{3}\frac{R^3}{r} - \tfrac{1}{6}r^2\right] \tag{24}$$

At point P_o on the geoid $r=R$, so we have

$$\begin{aligned} V'_{|P_o} &= 4\pi k\rho \left[\tfrac{1}{2}(R+h_p)^2 - \tfrac{1}{3}R^2 - \tfrac{1}{6}R^2\right] \\ &= 4\pi k\rho \left[\tfrac{1}{2}R^2 + Rh_p + \tfrac{1}{2}h_p^2 - \tfrac{1}{2}R^2\right] \\ &= 4\pi k\rho \left(Rh_p + \tfrac{1}{2}h_p^2\right) \\ &= 4\pi k\rho Rh_p(1+\tfrac{1}{2}u) \end{aligned} \tag{25}$$

Then we have the vertical attraction of the spherical shell at point P_o as:

$$\begin{aligned} A'_{|P_o} &= -\frac{\partial}{\partial R} V'_{|P_o} \\ &= -\frac{\partial}{\partial R} \left(4\pi k\rho Rh_p + 2\pi k\rho h_p^2\right) \\ &= -4\pi k\rho h_p \end{aligned} \tag{26}$$

For the potential of the condensed layer at point P_0 on the geoid, we consider that point P_0 is just outside the condensed layer so the layer acts like a point mass, i.e.,

$$V'_{s|P_0} = \frac{kM_s}{R}$$

$$= 4\pi k\rho R h_p \left(1+u+\tfrac{1}{3}u^2\right) \qquad (27)$$

The vertical attraction of the condensed layer at point P_0 on the geoid is:

$$A'_{s|P} = -\frac{kM_s}{R^2}$$

$$= -4\pi k\rho h_p \left(1+u+\tfrac{1}{3}u^2\right) \qquad (28)$$

A summary of expressions for computing the potentials and the vertical attractions of the spherical shell and the corresponding condensed layer at point P on the earth's surface and at point P_0 on the geoid is given in Table 1. Also shown in the table are the changes in potential and vertical attraction at points P and P_0.

Comparing the quantities of V', V'_s, A' and A'_s at point P on the earth's surface and point P_0 on the geoid, we see that the differences are in the order of u. Neglecting u-terms in the computation would cause a relative error smaller than 0.14% (Moritz, 1968, p. 4). To get an idea how large the difference of these quantities can be, we take an example of h_p = 3000 meters, R = 6371000 meters, Newtonian gravitational constant $k = 6.672 \times 10^{-11}$ $m^3/(kg\text{-}sec^2)$ and volume density $\rho = 2.67$ gm/cm^3 or 2.67×10^3 kg/m^3. The result is shown in Table 2.

From Table 2, using different evaluation points between P and P_0 gives differences of potentials in the order of 1-2 kgal-m and differences of vertical attractions in the order of 0.3-0.6 mgal for h_p = 3000 m. By Brun's formula of equation (2), the potential change of 1 kgal-m gives approximately the indirect effect on geoid undulation

Table 1: Potentials and vertical attractions of the masses of a spherical shell and the condensed mass onto the geoid at two evaluation points.

Quantities	Evaluated at P_o	Evaluated at P
V	$4\pi k\rho R h_p(1+\frac{u}{2})$	$\frac{kM_s}{R+h_p} = 4\pi k\rho R h_p(1+\frac{u^2}{3} - \frac{u^3}{3} + \dots)$
V'_s	$4\pi k\rho R h_p(1+u+\frac{u^2}{3})$	$4\pi k\rho R h_p(1+\frac{u^2}{3} - \frac{u^3}{3} + \dots)$
$V' - V'_s$	$-4\pi k\rho R h_p(\frac{u}{2}+\frac{u^2}{3}) =$ $[-2\pi k\rho h_p^2]$	0
A'	$-4\pi k\rho h_p$	$\frac{kM_s}{(R+h_p)^2} = -4\pi k\rho h_p(1-u+\frac{4u^2}{3} - \frac{5u^3}{3} + \dots)$
A'_s	$-4\pi k\rho h_p(1+u+\frac{u^2}{3})$	$-4\pi k\rho h_p(1-u+\frac{4u^2}{3} - \frac{5u^3}{3} + \dots)$
$A' - A'_s$	$4\pi k\rho h_p(u+\frac{u^2}{3})$	0

Note

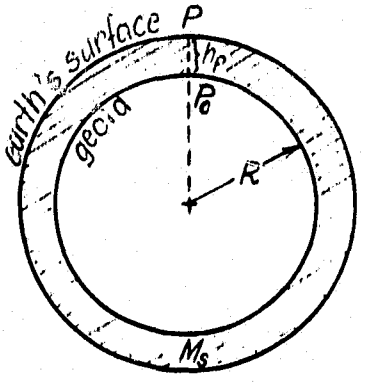

( )' = effect due to spherical shell

$( )'_s$ = effect due to the condensed layer

k = Newton's gravitational const.

M_s = mass of the spherical shell

ρ = density of the earth's crust

$u = \frac{h_p}{R}$

Table 2: Numerical example of Table 1 with h_p = 3000 m , R = 6,371 km , k = $6.67\,2 \times 10^{-11}$ $m^3/(kg\text{-}sec^2)$ and $\rho = 2.67 \times 10^3$ kg/m^3 .

Quantity (in unit)	Evaluated at P_o	Evaluated at P	Difference between two evaluation points
V' (kgal-m)	4279.6501	4278.6430	1.0071
V'_s (kgal-m)	4280.6578	4278.6430	2.0071
$V' - V'_s$ (kgal-m)	-1.0077	0	-1.0077
A' (mgal)	-671.5810	-671.2650	-0.3160
A'_s (mgal)	-671.8973	-671.2650	-0.6323
$A' - A'_s$ (mgal)	0.3163	0	0.3163

of 1 meter. Consider that the average terrain is lower than 3000m, we would normally have the differences less than the values shown in Table 2. In the past, the magnitudes of differences mentioned above can be tolerated. Therefore, this could be a reason that not much attention was given to seriously define the location of evaluation points for computing the potential change and the attraction change due to the second method of Helmert's condensation. Now we are talking about the computation of geoid undulation in the order of 10 centimeters, therefore, we need to define the exact location of the evaluation point. To do this let us follow the reduction process in the second method of Helmert's condensation step-by-step as follows, see also figure 1:

(a) We have gravity value, g_{obs} at point P on the earth's surface.

(b) Remove the topographic masses above the geoid. We compute the attraction, A_T at the point P caused by these masses and subtract from the observed value, g_{obs} .

(c) Bring the masses back and condense on the layer of the geoid. Here, we have to compute the attraction, A_C at the point P again which is caused by the condensed layer and add to the result in (b) .

(d) Transfer the gravity to point P_o on the geoid by a free-air reduction, F . For the point P above the geoid, F is added to the result in (c) .

(e) Compute a normal gravity, γ of the reference ellipsoid at corresponding point Q_o on the ellipsoid.

(f) We finally get

$$\Delta g_H = g_{obs} - A_{T|P} + A_{C|P} + F - \gamma_{|Q_o} \qquad (29)$$

The vertical line followed by a letter indicates the point where a particular function is evaluated.

The secondary indirect effect is assumed to be negligibly small and not included in the reduction procedure explained above. We can see from equation (29) that $g_{obs} + F - \gamma$ is in fact a free-air anomaly at the geoid and $(A_T - A_C)$ is the gravity attraction change due to the second method of Helmert's condensation and it is evaluated at point P on the earth's surface.

To determine the potential change in the reduction process, we realize that the indirect effect, δN on the geoid undulation is caused by the potential change, δW on the geoid due to the change of the position of the masses in the reduction process. Then we have to evaluate the potential change, δW at point P_o on the geoid.

We can conclude that the computation point or the evaluation point of the attraction change is at point P on the earth's surface and the computation point of the potential change is at point P_o on the geoid.

In the next section we will explore the change in gravitational potential due to the second method of Helmert's condensation, which will lead us to the indirect effect on geoid undulation.

2.1 Effect of the Second Method of Helmert's Condensation on Potential Change

The gravitational potential of the topographic masses at point P_0 is:

$$V = k \iiint \frac{dm}{\ell} \tag{30}$$

The integral is extended over the masses outside the geoid; dm is the element of mass and ℓ is the distance of mass dm from the evaluation point P_0, (See Figure 3). Let ρ be a volume density of the topographic masses and assumed to be a constant. Then equation (30) can be written as:

$$V = k\rho \iiint \frac{dv}{\ell} \tag{31}$$

where dv is the element of volume and the integral is extended over the exterior of the geoid. The element $dv = r^2 d\sigma dr$ where $d\sigma$ is the elements of solid angle and r is the distance between mass element dm and the center of the earth. By planar approximation,

$$dv = R^2 d\sigma dz$$

(see Figure 3) so that equation (31) becomes

$$V = k\rho R^2 \iint_{\sigma} \int_{z=0}^{h} \frac{d\sigma\, dz}{\ell}$$

where σ denotes solid angle over the whole sphere. We rewrite this equation again as

$$V = k\rho R^2 \iint_{\sigma} \int_{z=0}^{h_p} \frac{d\sigma dz}{\ell} + k\rho R^2 \iint_{\sigma} \int_{z=h_p}^{h} \frac{d\sigma dz}{\ell}$$

$$= V' + V'' \tag{32}$$

We see that V' represents the gravitational potential at point P_o of the plate which is called the regular part of topography. V'' represents the gravitational potential at point P_o of the masses above the plate and non-existing masses under the plate which are called the irregular part of topography or topographic variation. That is the potential of the topographic masses can be split into the potentials of the regular and irregular parts.

Similarly, the potential of the condensed layer after Helmert's condensation can also be split into two corresponding parts:

$$V_s = V_s' + V_s'' \tag{33}$$

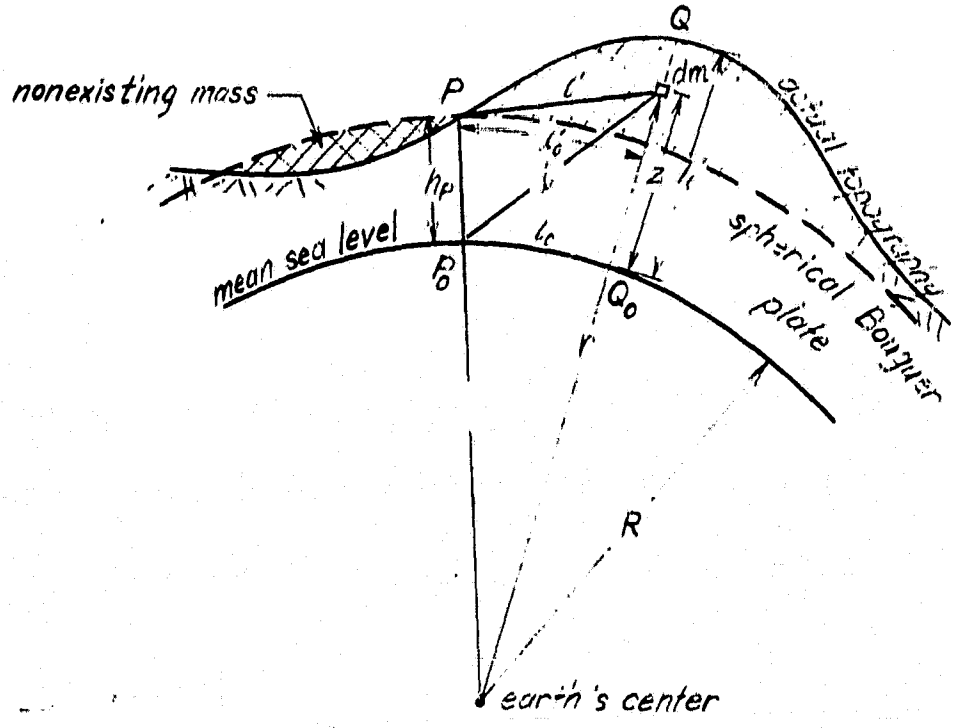

Figure 3: The regular part of topography is represented by a spherical Bouguer plate and the irregular part is represented by the masses above the plate and the non-existing masses under the plate (cross hatched areas in the figure).

Then the potential change at point P_0, δV in Helmert's condensation reduction can be written as

$$\delta V = V - V_s \tag{34}$$

$$= (V' + V'') - (V'_s + V''_s)$$

$$= (V' - V'_s) + (V'' - V''_s)$$

$$= \delta V' + \delta V'' \tag{35}$$

where $\delta V'$ represents the potential change of a regular part of topography and $\delta V''$ represents the potential change of an irregular one. Therefore, we can investigate the expressions for the potential changes of a regular part and an irregular part of topography separately.

2.1.1 Regular Part

As mentioned before, the effect of a regular part of topography or the Bouguer plate can be computed by different degrees of approximation. We start from the one that has the least degree of approximation.

(a) Spherical Bouguer Plate: The regular part of the topography is described as a portion of the spherical shell with thickness h_p and angular radius ψ from the computation point. The gravitational potential of this topographic mass at point P_0 on the geoid can be written as follows (Baeschlin, 1948, p. 519) and (Lambert and Darling, 1936, p. 6):

$$V' = \pi k\rho R^2 \{\sin^2\psi\,[f(\psi, h_p) - f(\psi, 0)] + 4B_0\} \tag{36}$$

where

$$f(\psi,x) = \frac{2\sin\psi}{3\cos^3\gamma} + \frac{\cos\psi\,\tan\gamma}{\cos\gamma} + \cos\psi\,\ell n\,\tan\left(\frac{\pi}{4} + \frac{\gamma}{2}\right)$$

with

$$\tan\gamma = \tan\frac{\psi}{2} + \frac{x}{R\sin\psi} \tag{37}$$

The angle ψ is the angular radius of the plate subtended at the center of the sphere (see Figure 4), and B_0 is defined below.

The gravitational potential of a spherical Bouguer plate can also be expressed in hyperbolic functions as (Baeschlin, 1948, eq. 75.27; and Lambert and Darling, 1936, eq. 28c):

$$V' = 4\pi k\rho R^2\{B_0+\tfrac{1}{6}\sin^3\psi(\cosh^3\phi_2 - \cosh^3\phi_1)$$

$$+ \tfrac{1}{4}\sin^2\psi\cos\psi(\phi_2-\phi_1)$$

$$+ \tfrac{1}{4}\sin^2\psi\cos\psi(\sinh\phi_2\cosh\phi_2 - \sinh\phi_1\cosh\phi_1)\} \qquad (38)$$

with

$$B_0 = -\tfrac{1}{4}\left(\frac{h_p}{R}\right)\left[1 + \tfrac{2}{3}\left(\frac{h_p}{R}\right)\right]$$

$$\sinh\phi_1 = \tan\frac{\psi}{2}$$

$$\sinh\phi_2 = \tan\frac{\psi}{2} + \frac{h_p}{R\sin\psi} \qquad (39)$$

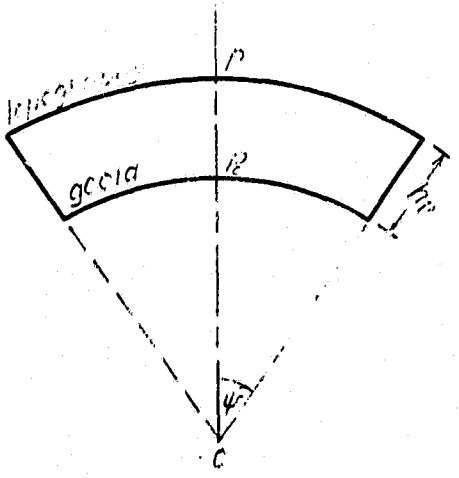

Figure 4: Topography is represented by a spherical Bouguer plate

To obtain the gravitational potential of the condensed layer, we make use of the expression for the potential of a spherical disk given

by Baeschlin (1948, equation 75.17) as:

$$V' = 2\pi k\rho dr \frac{r}{R} (E-z)$$

with $E = \sqrt{R^2 + r^2 - 2Rr\cos\psi}$ where r is the distance from the center of the earth to the evaluation point, dr is the thickness of the disk and $z = r-R$. To apply the above equation to the condensed layer of a spherical Bouguer plate of height h_p, we replace dr by h_p and with the evaluation point at P_0 on the geoid, we have $r=R$ and $z=0$ then,

$$E = \sqrt{R^2 + R^2 - 2R^2\cos\psi}$$

$$= R\sqrt{2 - 2\cos\psi} \quad .$$

With the trigonometric identity $(1-\cos\psi) = 2\sin^2\frac{\psi}{2}$ we get

$$E = 2R \sin\frac{\psi}{2} \quad .$$

So we can write the potential of the condensed layer of the spherical Bouguer plate at point P_0 as

$$V'_s = 4\pi k\rho h_p R \sin\frac{\psi}{2} \qquad (40)$$

Therefore we can compute the potential change at point P_0 of spherical Bouguer plate with equation (36) or (38) and equation (40).

Next we turn to a less accurate way to estimate the potential of the regular topography.

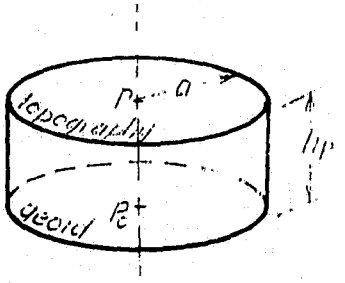

Figure 5: Topography is represented by a plane circular plate

(b) Plane Circular Plate: Here, the regular part of the topography is a flat plate with thickness h_p and linear radius a from the computation point. The expression for the graviational potential of the plate is less complicated than the pontential of the spherical Bouguer plate. The potential of the plane circular plate at point P_o is given by (Heiskanen and Moritz, 1967, p. 128; Baeschlin, 1948, p. 500):

$$V' = \pi k\rho[-h_p^2 + h_p E_1 + a^2 \ell n \frac{h_p+E_1}{a}] \tag{41}$$

with $E_1 = \sqrt{a^2 + h_p^2}$ (see Figure 5). For an equivalent area with the spherical plate in (a), the linear radius of the plane plate is:

$$a = 2R \sin\frac{\psi}{2} \tag{42}$$

Using equation (3-9) of Heiskanen and Moritz (1967) and letting quantity c which is the height of the evaluation point equal to zero; we get the potential of the condensed layer of the plane circular plate at point P_o as:

$$\begin{aligned} V_s' &= 2\pi k\kappa a \\ &= 2\pi k\rho h_p (2R \sin\frac{\psi}{2}) \\ &= 4\pi k\rho h_p R \sin\frac{\psi}{2} \end{aligned} \tag{43}$$

Comparing equation (43) with equation (40), we see that the potentials of the condensed layers of the equivalent size of plates are the same regardless of a spherical or a flat plate.

Finally, we turn to the least accurate approximation for the regular topography.

(c) Infinite Plane Plate or Plane Bouguer Plate: This is the plane circular plate of height h_p in (b) with a radius of infinity. Grushinsky (1969, p. 210) gives for the potential of the infinite plate at point P_o:

$$V' = 2\pi k\rho h_p a [1 - \frac{h_p}{2a} + (\frac{h_p}{2a})^2]$$

and the corresponding potential for the condensed topography is:

$$V_s' = 2\pi k\rho h_p \cdot a$$

Of specific interest, here is the difference $V' - V_s'$ (see eq. 35) which can be simply computed for model (c) but not models (a) and (b). We have:

$$\delta V' = -2\pi k\rho h_p \cdot a \left[\frac{h_p}{2a} - \left(\frac{h_p}{2a}\right)^2\right]$$

$$= -\pi k\rho h_p^2 + \frac{\pi k\rho h_p^3}{2a}$$

As the radius a approaches infinity, the second term in the equation goes to zero, so we have

$$\delta V' = -\pi k\rho h_p^2 \tag{44}$$

Equation (44) will be referred to later as Grushinsky's formula.

2.1.2 Irregular Part

The gravitational potential at point P_0 of the irregular part of topography is defined to be (equation (32)):

$$V'' = k\rho R^2 \iint_{\sigma} \int_{z=h_p}^{h} \frac{dz d\sigma}{\ell} \tag{45}$$

To solve equation (45), we consider the planar approximation of the topography shown in Figure 6. From the figure we have

$$\ell^2 = \ell_0^2 + z^2 \tag{46}$$

or we can write

$$\frac{1}{\ell} = \frac{1}{\ell_0}\left(1 + \frac{z^2}{\ell_0^2}\right)^{-\frac{1}{2}}$$

Expand the expression in parenthesis as a binomial series, we get

$$\frac{1}{\ell} = \frac{1}{\ell_0}\left(1 - \tfrac{1}{2}\frac{z^2}{\ell_0^2} + \tfrac{3}{8}\frac{z^4}{\ell_0^4} - \tfrac{15}{48}\frac{z^6}{\ell_0^6} + \ldots\right)$$

$$= \frac{1}{\ell_0} - \tfrac{1}{2}\frac{z^2}{\ell_0^3} + \tfrac{3}{8}\frac{z^4}{\ell_0^5} - \tfrac{15}{48}\frac{z^6}{\ell_0^7} + \ldots)$$

Substitute $1/\ell$ into equation (45) and integrate to obtain

$$V'' = V_1 + V_2 + V_3 + V_4 + \ldots \tag{47}$$

with

$$V_1 = k\rho R^2 \iint_\sigma \int_{z=h_p}^{h} \frac{dz\,d\sigma}{\ell_0}$$

$$= k\rho R^2 \iint_\sigma \frac{z}{\ell_0}\Big|_{z=h_p}^{h} d\sigma$$

$$= k\rho R^2 \iint_\sigma \frac{h-h_p}{\ell_0}\, d\sigma \tag{48}$$

$$V_2 = k\rho R^2 \iint_\sigma \int_{z=h_p}^{h} -\tfrac{1}{2}\frac{z^2}{\ell_0^3}\, dz\, d\sigma$$

$$= -\tfrac{1}{2} k\rho R^2 \iint_\sigma \tfrac{1}{3}\frac{z^3}{\ell_0^3}\Big|_{z=h_p}^{h} d\sigma$$

$$= -\tfrac{1}{6} k\rho R^2 \iint_\sigma \frac{h^3-h_p^3}{\ell_0^3}\, d\sigma \tag{49}$$

$$V_3 = k\rho R^2 \iint_\sigma \int_{z=h_p}^{h} \tfrac{3}{8}\frac{z^4}{\ell_0^5}\, dz\, d\sigma$$

$$= \tfrac{3}{40} k\rho R^2 \iint_\sigma \frac{h^5-h_p^5}{\ell_0^5}\, d\sigma \tag{50}$$

$$V_4 = k\rho R^2 \iint_\sigma \int_{z=h_p}^{h} -\tfrac{15}{48}\frac{z^6}{\ell_0^7}\, dz\, d\sigma$$

$$= -\tfrac{15}{336} k\rho R^2 \iint_\sigma \frac{h^7-h_p^7}{\ell_0^7}\, d\sigma \tag{51}$$

etc.

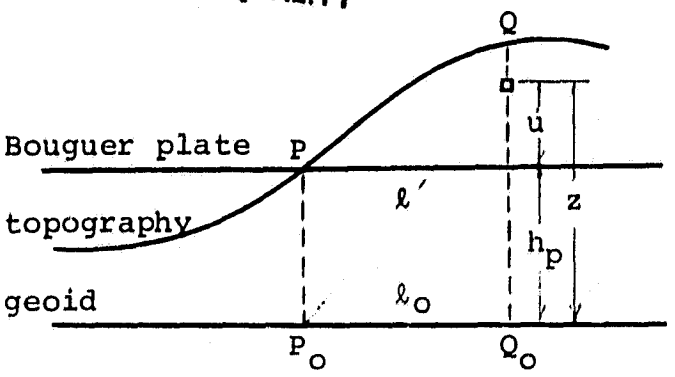

Figure 6: Topography in the planar approximation. The geoid may be visualized as a flat plate (Moritz, 1966, p. 33). The regular part of the topography is then visualed as the plane Bouguer plate.

Equation (47) with equations (48) to (51) resembles equation (22) of Moritz (1968) where he derives the gravitational potential at point P on the earth's surface of the irregular part of topography:

$$V''|_P = V_1^* + V_2^* + V_3^* + \ldots \tag{52}$$

where

$$V_1^* = k\rho R^2 \iint_\sigma \frac{h-h_p}{\ell_0'}\, d\sigma$$

$$V_2^* = -\tfrac{1}{6} k\rho R^2 \iint_\sigma \frac{(h-h_p)^3}{\ell_0'^3}\, d\sigma \tag{53}$$

$$V_3^* = \tfrac{3}{40} k\rho R^2 \iint_\sigma \frac{(h-h_p)^5}{\ell_0'^5}\, d\sigma$$

etc.

The distance ℓ_0' can be seen in Figure 3 on page 20.

The potential of a surface layer at point P_0 on the geoid is given by (Heiskanen and Moritz, 1967, eq. 1-16):

$$V_s = k \iint_\sigma \frac{K}{\ell_0} R^2\, d\sigma \tag{54}$$

where κ is the surface density of the layer. Applying this equation to the irregular part of the topography, we have surface density $\kappa = \rho(h-h_p)$. Then the potential of the condensed layer of the irregular part at point P_o is:

$$V_s'' = k \iint_\sigma \frac{\rho(h-hp)}{\ell_0} R^2 \, d\sigma$$
$$= k\rho R^2 \iint_\sigma \frac{h-hp}{\ell_0} \, d\sigma \qquad (55)$$

We see that V_s'' is equal to V_1 term of equation (47) so that $\delta V''$ $(=V''-V_s'')$ is:

$$\delta V'' = V_2 + V_3 + V_4 + \ldots \qquad (56)$$

Therefore, equation (56) in conjunction with the potential change of either model (a), (b) or (c) in subsection 2.1.1 can be used to obtain the total potential change due to the second method of Helmert's condensation.

In the next section we will look at the effect of the second method of Helmert's condensation on the attraction change.

2.2 Effect of the Second Method of Helmert's Condensation on Attraction Change

By definition, the vertical gravitational attraction at point P on the surface is written as:

$$A = - \frac{\partial V_{|P}}{\partial r_p}$$

where $V_{|P}$ is the gravitational potential at point P and r_p represents the vertical direction at point P for the spherical approximation of the geoid. Comparable to equation (32), we may separate the gravitational attraction of actual topography into two parts. Since $V = V' + V''$, then

$$A = -\frac{\partial V'|_P}{\partial r_p} - \frac{\partial V''|_P}{\partial r_p} = A' + A'' \tag{57}$$

Similarly, the attraction of the condensed layer at point P can be written as

$$A_s = A_s' + A_s'' \tag{58}$$

Then the difference of gravitational attraction between the topography and the condensed layer at point P is:

$$A_T - A_C = \delta A = A - A_s$$

$$= (A' + A'') - (A_s' + A_s'') \tag{59}$$

$$= (A' - A_s') + (A'' - A_s'') \tag{60}$$

$$= \delta A' + \delta A''$$

Therefore $\delta A'$ represents the attraction change of a regular part of topography and $\delta A''$ represents that of an irregular one. So we will investigate the attraction change of the regular part of topography separate from the attraction change of the irregular one.

2.2.1 Regular Part

The attraction change of the regular part may be computed in three different ways as follows:

(a) Spherical Bouguer Plate: The attraction of the topography at point P on the earth's surface given by Baeschlin (1948, p. 529) is

$$A' = -2\pi k\rho R \sin\psi\{(\cosh\phi + \sinh\phi)\left(\frac{r}{R}\cos\psi + \frac{1}{3}\sin^2\psi \sinh^2\phi\right)$$

$$- \frac{2}{3}\sin^2\psi \cosh\phi - \sin\psi \cos\psi\,\phi\}_{\phi_1}^{\phi_2} \tag{61}$$

with

$$\sinh\phi = \frac{r - R\cos\psi}{R\sin\psi}; \qquad \phi_1 : r = R$$

$$\phi_2 : r = R + h_p \tag{62}$$

The expressions for $\sinh\phi_1$ and $\sinh\phi_2$ in equation (62) can be easily reduced to the corresponding expressions in equation (39). The attraction of the corresponding condensed topography at the point P is

$$A_s' = 2\pi k\rho h_p \left(\frac{R}{R+h_p}\right)^2 \left\{1 - \frac{(R+h_p)\cos\psi - R}{E}\right\} \tag{63}$$

where

$$E = \sqrt{(R+h_p)^2 + R^2 - 2R(R+h_p)\cos\psi} \tag{64}$$

The attraction change of a regular part of the topography is then calculated from

$$\delta A' = A' - A_s' \quad .$$

(b) Plane Circular Plate: The attraction of the actual topography at point P on the earth's surface given by Heiskanen and Moritz (1967, eq. 3-6) is:

$$A' = 2\pi k\rho \left(a + h_p - \sqrt{a^2 + h_p^2}\right) \tag{65}$$

and the attraction of the condensed topography at the point P is (Ibid., eq. 3-10):

$$A_s' = 2\pi k\rho h_p \left(1 - \frac{h_p}{\sqrt{a^2 + h_p^2}}\right) . \tag{66}$$

(c) Infinite Plane Plate: The attraction change of the infinite plane plate or Bouguer plate is zero. This can be verified by equations (65) and (66) taking $a \to \infty$. We can write equation (65) as

$$A' = 2\pi k\rho \left(h_p + a - a\sqrt{1 + \left(\frac{h_p}{a}\right)^2}\right)$$

With $a \to \infty$, $\frac{h_p}{a} \to 0$ and $\frac{h_p}{\sqrt{a^2 + h_p^2}} \to 0$, the above equation becomes

$$A' = 2\pi k\rho h_p$$

and equation (66) becomes

$$A'_S = 2\pi k\rho h_P \ .$$

Therefore,

$$\delta A' = A' - A'_S = 0 \ .$$

Next we turn to the attraction change of the irregular part of topography.

2.2.2 Irregular Part

The total attraction change (sum of the attraction change of the regular part and that of the irregular part) at point P on the earth's surface in the second method of Helmert's condensation is given by Moritz (1968, eq. 63) to be:

$$\delta A = A - A_S = - C \tag{67}$$

where C is the quantity called the "terrain correction". By the planar approximation (Ibid., eq. 42),

$$C = \tfrac{1}{2} k\rho R^2 \iint_\sigma \frac{(h-h_P)^2}{\ell_0'^3} \, d\sigma \tag{68}$$

In his derivation, Moritz uses a spherical shell as a regular part of topography (Ibid., p. 6). If we examine the derivation, we can see that the total amount of attraction change (-C) comes from the attraction change of the irregular part alone. This argument is strengthened by the fact that the attraction change of a spherical shell at point P on the earth's surface is zero (see Table 1 on page 16) i.e., we have

$$\delta A'' = - C \tag{69}$$

It should be noted here that the masses further away from the evaluation point P contribute a very small effect on the terrain correction.

The effect decreases very rapidly as we can see from the term ℓ_0^3 in the denominator of equation (68).

Using equation (69) and the attraction change of the regular part (model (a) or (b) in subsection 2.2.1), we arrive at the total attraction change within a certain cap size. This statement does not contradict the statement we just made that the attraction change of the regular part of topography for the whole spherical shell is zero. In practice, we do not integrate over the whole sphere. We usually consider the effect (e.g., the effect of gravity anomalies on the geoid undulations) within a certain cap size, for example, 10° or 20° from the evaluation point. To compute the attraction change we may also have to consider the effect of the topography only within the cap size.

In the next section, we will compute the numerical values of the potentials and attractions presented here. Then we will make a comparison so that the conclusion concerning which expressions we should use to obtain the most accurate geoid computation can be made.

2.3 Comparison of Formulas Using Simple Test Models

As discussed earlier, the regular part of the topography may be represented by at least three models, i.e. the spherical Bouguer plate, the plane circular plate and the infinite plane plate. We, then, want to know whether it makes any difference to use one model instead of another and whether there should be limitations to do so or not. Moreover, based on the expressions for computing the potential change and the attraction change of the irregular part of the topography, we would like to know if these expressions have any relations with the expressions for the regular part.

The topographic masses above the sea level occur in about 30% of the total area of the surface of the earth. Masses further away from the compuation point have very small effects on the values of the potential

change and the attraction change. It would then be more appropriate if we used the regular part of the topography at a certain cap size to cover a particular continental area only. This is because there are no topographic masses above the geoid to be condensed in the ocean area. Thus the effects on the potential change and the attraction change at any evaluation point computed from ocean area masses are zero. By selecting one cap size for the whole area we may however take too much mass into account in the computation of the regular part. If it is possible, then we would like to see that the effect computed from the irregular part will compensate for the excessive effect from the regular part.

To investigate the numerical effect on the potential change and the attraction change of the regular part of topography, spherical Bouguer plates with height h varying from 500m to 9000m and angular radii ψ varying from 1° to 180° are used in this study for the expressions of model (a) in subsections 2.1.1 and 2.2.1. Plane circular plates with the same heights and radii as those of spherical Bouguer plates are used for the expressions of model (b) in subsections 2.1.1 and 2.2.1. The same size of the plate in each model is used so that we can compare the effects on potential change and attraction change.

To compare the effects on potential change and attraction change of the regular part with those of the irregular part, we use a "spherical ring" and a "cylindrical ring" (see Figure 7). A spherical ring is a portion of a spherical Bouguer plate which is bounded by angular radii ψ_1 and ψ_2 while a cylindrical ring is a portion of a plane circular plate bounded by linear radii a_1 and a_2.

The potential change at point P_0 of a spherical ring can be computed from the difference between the potential changes of spherical Bouguer plates of angular radii ψ_1 and ψ_2 explained in subsection 2.1.1(a). Similarly, the attraction change at point P of a spherical ring is computed from the difference between the attraction changes of spherical Bouguer plates of radii ψ_1 and ψ_2 explained in subsection 2.2.1(a). This method of computing the potential change and attraction change from two different radius of spherical Bouguer plates will be referred to

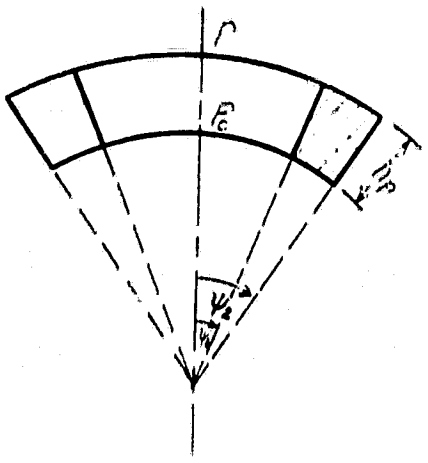

(a) A section of a spherical ring

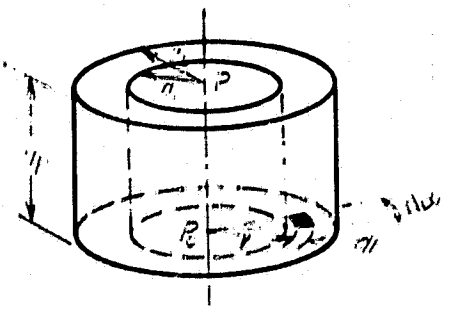

(b) A cylindrical ring

Figure 7: Models for comparison between the effects on the potential change and the attraction change of the regular part and the irregular part of the topography.

later as TDSBP (Two Different Spherical Bouguer Plate) method.

The potential change at point P_0 of a cylindrical ring can be computed from the difference between the potential changes of plane circular plates of linear radii a_1 and a_2 explained in subsection 2.1.1(b). The attraction change at point P of a cylindrical ring is computed from the difference between the attraction changes of plane circular plates of radii a_1 and a_2 explained in subsection 2.2.1(b). The method of computation here will be referred to as TDPCP (Two Different Plane Circular Plate) method.

The potential change of the irregular part of topography (equation (56) with equations (49) to (51) in subsection 2.1.2) can also be used to compute the potential change of a cylindrical ring as follows: From equation (49),

$$V_2 = -\frac{1}{6} k\rho \iint_{\sigma} \frac{h^3 - h_p^3}{\ell_0^3} R^2 \, d\sigma$$

For a cylindrical ring, h is constant and we have $R^2 d\sigma = r d\alpha dr$ and $\ell_0 = r$ (see Figure 7 (b)). So we can write

$$\begin{aligned} V_2 &= -\tfrac{1}{6} k\rho \, (h^3 - h_p^3) \int_{r=a_1}^{a_2} \int_{\alpha=0}^{2\pi} d\alpha \, \frac{r dr}{r^3} \\ &= -\frac{2\pi k\rho}{6} (h^3 - h_p^3) \int_{r=a_1}^{a_2} \frac{dr}{r^2} \\ &= -\tfrac{1}{3} \pi k\rho \, (h^3 - h_p^3) \left(-\frac{1}{r}\right)\Big|_{r=a_1}^{a_2} \\ &= -\tfrac{1}{3} \pi k\rho \, (h^3 - h_p^3) \left(\frac{a_2 - a_1}{a_1 a_2}\right) \end{aligned} \tag{70}$$

Similary, V_3 and V_4 terms for a cylindrical ring with height h and radii a_1, a_2 can be computed directly from

$$V_3 = \tfrac{1}{20} \pi k\rho \, (h^5 - h_p^5) \left(\frac{a_2^3 - a_1^3}{a_1^3 a_2^3}\right) \tag{71}$$

and

$$V_4 = -\tfrac{3}{168} \pi k\rho \, (h^7 - h_p^7) \left(\frac{a_2^5 - a_1^5}{a_1^5 a_2^5}\right) \tag{72}$$

The attraction change of the irregular part of topography is equal to the negative value of the terrain correction. Equation (69) with equation (68) can also be used to compute the attraction change of a cylindrical ring. By the same algebraic manipulation used for V_2, V_3 and V_4 terms, we can write

$$\delta A'' = -\pi k\rho\ (h-h_p)^2\ \left(\frac{a_2-a_1}{a_1 a_2}\right) \tag{73}$$

The method of computing the potential change and attraction change of a cylindrical ring by using the expressions for the irregular part of topography explained above will be referred to as an integration method.

A spherical ring and a cylindrical ring are called identical if the linear radius of the cylindrical ring is related to the angular radius of the spherical ring by equation (42) and the heights of both rings are equal. By using the identical ring in TDSBP, TDPCP and the integration method, we can compare the values of the potential changes and the attraction changes. Then we may find a relation between the expressions of the regular part and the expressions of the irregular part for the potential change and the attraction change.

The next subsection is the numerical results in computing the potential change using the various expressions explaiend above.

2.3.1 Comparison of Formulas for Potential Change

The potential change in the second method of Helmert's condensation is the difference between the potential of the topography and the potential of the condensed layer, evaluated at point P_0 on the geoid. The potential change at point P_0 on the geoid of a plane circular plate as computed from equations (41) and (43) are negative. Its values become more negative when the thickness of the plate increases. It is approximately a parabolic function of the thickness or the height of the plate. Figure 8 shows the typical relation between the potential change, $\delta V'$ and the height, h_p of a plane circular plate when the radius of the plate is held fixed.

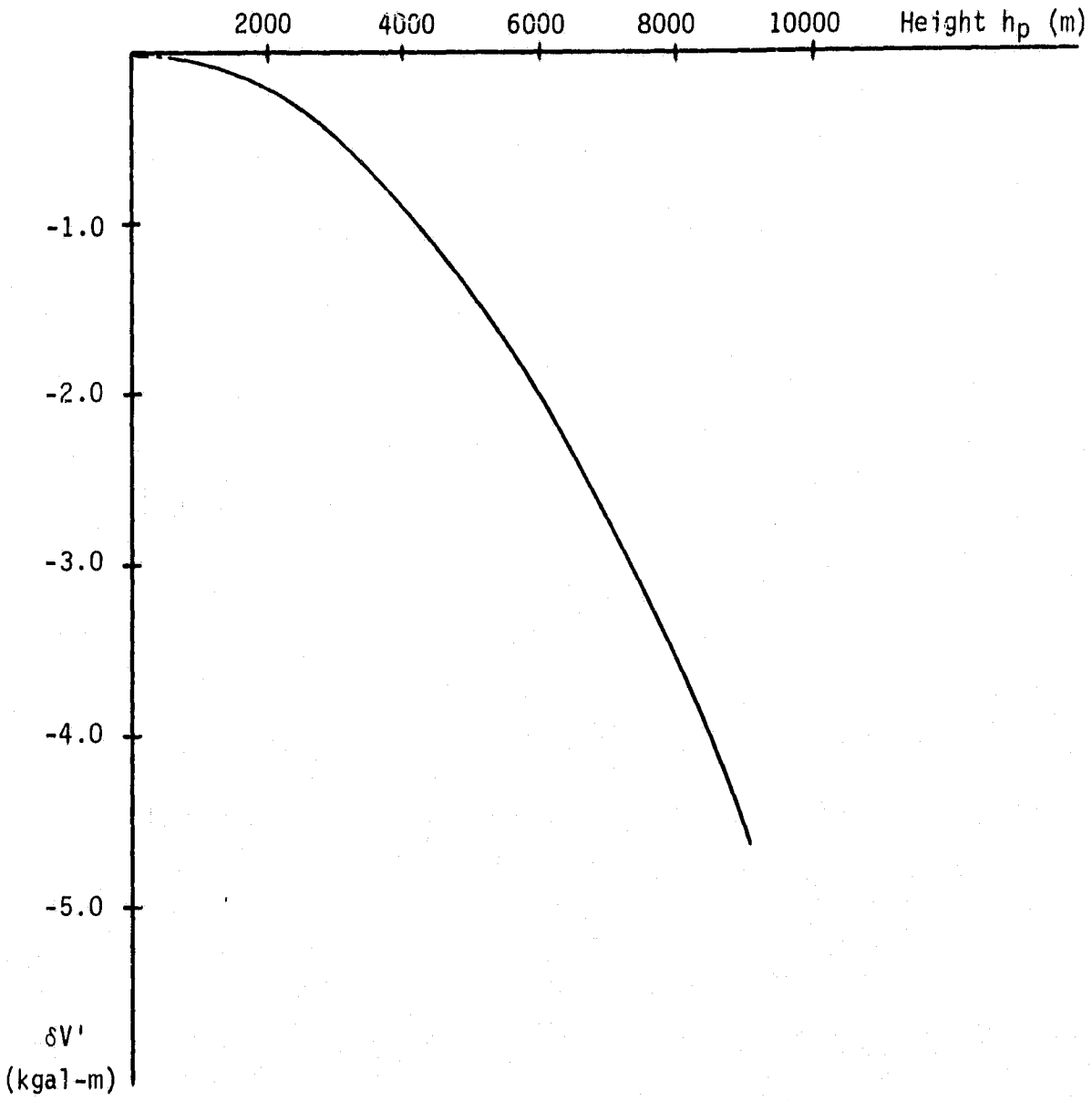

Figure 8: Relation between the potential change, $\delta V'$ of the plane circular plate with $\psi = 5°$ and height h_p in the second method of Helmert's condensation.

The numerical values of $\delta V'$ in Figure 8 are obtained for the radius of the plate being 5° and the earth radius, R being 6,371 kilometers.

The potential change at the point P_o of a plane circular plate is also more negative when the radius of the plate increases and the height of the plate is held fixed. However, the value of the potential change is changing very slowly in this case. As we already discussed in subsection 2.1.1, an infinite plane plate is a special case of a plane circular plate where the radius of a circular plate is extended to infinity. Subsequently, we should expect that as the radius of a plane circular plate becomes larger, the value of the potential change of the plate approaches the value computed from Grushinsky's formula (equation (44)) which is the potential change of the infinite plane plate. This intuition is true as we can see from Table 3. Table 3 shows the potential change of a plane circular plate in relation to height h_p from 500 m to 9000 m and to angular radius from 1° to 20°, along with the value computed by Grushinsky's formula. Table 4 gives the potential change error in percents if we were to use Grushinsky's formula to compute potential change instead of using a certain size of a plane circular plate. For example, if we use Grushinsky's formula for the plate of height 3000 m, the potential change is -0.504 kgal-meter or the indirect effect on geoid undulation is about -50 cm. Suppose that the plane circular plate of 5° radius should be used instead of using Grushinsky's formula in the computation. We have the relative error of 0.2% which is equal to 0.1 cm in computation. In this particular example we see that the difference between the two expressions is insignificant for the geoid accuracy of 10 cm. Even in the extreme case when the height of the terrain is 9000 m above the geoid, the error in using Grushinsky's formula to compute the potential change at point P_o is less than 3 cm. We can, then, say that Grushinsky's formula may be used as an approximation to compute the potential change at point P_o of the plane circular plate.

The potential change of a spherical Bouguer plate at the point P_o is compute from equations (36) and (40). The value of the potential change of a spherical Bouguer plate starts with nearly the same negative

Table 3: Potential change at point P_0 (in kgal-m) of a plane circular plate as computed from equations (41) and (43) and that of an infinite plane plate as computed from Grushinsky's formula (equation (44)).

HEIGHT	ANGULAR RADIUS OF THE PLATE (DEGREES)										GRUSHINSKY
(M.)	1	2	3	4	5	6	7	8	9	10	FORMULA
500	-0.014	-0.014	-0.014	-0.014	-0.014	-0.014	-0.014	-0.014	-0.014	-0.014	-0.014
1000	-0.056	-0.056	-0.056	-0.056	-0.056	-0.056	-0.056	-0.056	-0.056	-0.056	-0.056
1500	-0.125	-0.126	-0.126	-0.126	-0.126	-0.126	-0.126	-0.126	-0.126	-0.126	-0.125
2000	-0.223	-0.223	-0.223	-0.224	-0.224	-0.224	-0.224	-0.224	-0.224	-0.224	-0.224
2500	-0.347	-0.348	-0.349	-0.349	-0.349	-0.349	-0.349	-0.349	-0.349	-0.350	-0.350
3000	-0.499	-0.501	-0.502	-0.503	-0.503	-0.503	-0.503	-0.503	-0.503	-0.503	-0.504
3500	-0.678	-0.682	-0.683	-0.684	-0.684	-0.684	-0.685	-0.685	-0.685	-0.685	-0.686
4000	-0.885	-0.890	-0.892	-0.893	-0.893	-0.894	-0.894	-0.894	-0.894	-0.894	-0.895
4500	-1.118	-1.126	-1.128	-1.129	-1.130	-1.131	-1.131	-1.131	-1.132	-1.132	-1.133
5000	-1.378	-1.389	-1.392	-1.394	-1.395	-1.396	-1.396	-1.397	-1.397	-1.397	-1.399
5500	-1.665	-1.679	-1.684	-1.686	-1.687	-1.688	-1.689	-1.689	-1.690	-1.690	-1.693
6000	-1.979	-1.997	-2.003	-2.006	-2.007	-2.009	-2.010	-2.010	-2.011	-2.011	-2.015
6500	-2.318	-2.341	-2.349	-2.353	-2.355	-2.357	-2.358	-2.359	-2.359	-2.360	-2.365
7000	-2.685	-2.714	-2.723	-2.728	-2.731	-2.733	-2.734	-2.735	-2.736	-2.737	-2.742
7500	-3.077	-3.113	-3.124	-3.130	-3.134	-3.136	-3.138	-3.139	-3.140	-3.141	-3.148
8000	-3.496	-3.539	-3.553	-3.560	-3.565	-3.567	-3.569	-3.571	-3.572	-3.573	-3.582
8500	-3.941	-3.992	-4.009	-4.018	-4.023	-4.026	-4.029	-4.031	-4.032	-4.033	-4.043
9000	-4.411	-4.472	-4.492	-4.503	-4.509	-4.513	-4.516	-4.518	-4.520	-4.521	-4.533

Table 3: (continued)

HEIGHT (M.)	ANGULAR RADIUS OF THE PLATE (DEGREES)										CRUSHINSKY FORMULA
	11	12	13	14	15	16	17	18	19	20	
500	-0.014	-0.014	-0.014	-0.014	-0.014	-0.014	-0.014	-0.014	-0.014	-0.014	-0.014
1000	-0.056	-0.056	-0.056	-0.056	-0.056	-0.056	-0.056	-0.056	-0.056	-0.056	-0.056
1500	-0.126	-0.126	-0.126	-0.126	-0.126	-0.126	-0.126	-0.126	-0.126	-0.126	-0.126
2000	-0.224	-0.224	-0.224	-0.224	-0.224	-0.224	-0.224	-0.224	-0.224	-0.224	-0.224
2500	-0.350	-0.350	-0.350	-0.350	-0.350	-0.350	-0.350	-0.350	-0.350	-0.350	-0.350
3000	-0.503	-0.503	-0.503	-0.503	-0.503	-0.503	-0.503	-0.503	-0.503	-0.503	-0.504
3500	-0.685	-0.685	-0.685	-0.685	-0.685	-0.685	-0.685	-0.685	-0.685	-0.685	-0.686
4000	-0.894	-0.895	-0.895	-0.895	-0.895	-0.895	-0.895	-0.895	-0.895	-0.895	-0.895
4500	-1.132	-1.132	-1.132	-1.132	-1.132	-1.132	-1.132	-1.132	-1.132	-1.133	-1.133
5000	-1.397	-1.397	-1.398	-1.398	-1.398	-1.398	-1.398	-1.398	-1.398	-1.398	-1.399
5500	-1.690	-1.691	-1.691	-1.691	-1.691	-1.691	-1.691	-1.691	-1.691	-1.692	-1.693
6000	-2.011	-2.012	-2.012	-2.012	-2.012	-2.012	-2.013	-2.013	-2.013	-2.013	-2.015
6500	-2.360	-2.361	-2.361	-2.361	-2.361	-2.362	-2.362	-2.362	-2.362	-2.362	-2.365
7000	-2.737	-2.737	-2.738	-2.738	-2.738	-2.739	-2.739	-2.739	-2.739	-2.739	-2.742
7500	-3.142	-3.142	-3.143	-3.143	-3.143	-3.144	-3.144	-3.144	-3.144	-3.144	-3.148
8000	-3.574	-3.575	-3.575	-3.576	-3.576	-3.576	-3.577	-3.577	-3.577	-3.577	-3.582
8500	-4.034	-4.035	-4.036	-4.036	-4.037	-4.037	-4.037	-4.038	-4.038	-4.038	-4.043
9000	-4.522	-4.523	-4.524	-4.524	-4.525	-4.526	-4.526	-4.526	-4.527	-4.527	-4.533

Table 4: Potential change error of Grushinsky's formula (equation(44)) when compared to result for a plane circular plate (in percents).

HEIGHT (M.)	ANGULAR RADIUS OF THE PLATE (DEGREES)										δV' FROM GRUSHINSKY'S FORMULA (kgal-m)
	1	2	3	4	5	6	7	8	9	10	
500	0.2	0.1	0.0	0.0	0.0	0.0	0.0	0.0	0.0	0.0	-0.014
1000	0.3	0.2	0.1	0.1	0.1	0.1	0.0	0.0	0.0	0.0	-0.036
1500	0.5	0.2	0.2	0.1	0.1	0.1	0.1	0.1	0.1	0.0	-0.126
2000	0.6	0.3	0.2	0.2	0.1	0.1	0.1	0.1	0.1	0.1	-0.224
2500	0.8	0.4	0.3	0.2	0.2	0.1	0.1	0.1	0.1	0.1	-0.350
3000	0.9	0.5	0.3	0.2	0.2	0.2	0.1	0.1	0.1	0.1	-0.504
3500	1.1	0.5	0.4	0.3	0.2	0.2	0.2	0.1	0.1	0.1	-0.686
4000	1.2	0.6	0.4	0.3	0.2	0.2	0.2	0.2	0.1	0.1	-0.895
4500	1.4	0.7	0.5	0.3	0.3	0.2	0.2	0.2	0.2	0.1	-1.133
5000	1.5	0.8	0.5	0.4	0.3	0.3	0.2	0.2	0.2	0.2	-1.399
5500	1.7	0.8	0.6	0.4	0.3	0.3	0.2	0.2	0.2	0.2	-1.693
6000	1.8	0.9	0.6	0.5	0.4	0.3	0.3	0.2	0.2	0.2	-2.015
6500	2.0	1.0	0.7	0.5	0.4	0.3	0.3	0.2	0.2	0.2	-2.365
7000	2.1	1.1	0.7	0.5	0.4	0.4	0.3	0.3	0.2	0.2	-2.742
7500	2.3	1.1	0.8	0.6	0.5	0.4	0.3	0.3	0.3	0.2	-3.148
8000	2.5	1.2	0.8	0.6	0.5	0.4	0.3	0.3	0.3	0.2	-3.582
8500	2.6	1.3	0.9	0.6	0.5	0.4	0.4	0.3	0.3	0.3	-4.043
9000	2.8	1.4	0.9	0.7	0.5	0.5	0.4	0.3	0.3	0.3	-4.533

Table 4: (continued)

HEIGHT (M.)	ANGULAR RADIUS OF THE PLATE (DEGREES)										δV' FROM GRUSHINSKY'S FORMULA (k-gal-m)
	11	12	13	14	15	16	17	18	19	20	
500	0.0	0.0	0.0	0.0	0.0	0.0	0.0	0.0	0.0	0.0	-0.014
1000	0.0	0.0	0.0	0.0	0.0	0.0	0.0	0.0	0.0	0.0	-0.056
1500	0.0	0.0	0.0	0.0	0.0	0.0	0.0	0.0	0.0	0.0	-0.126
2000	0.1	0.1	0.0	0.0	0.0	0.0	0.0	0.0	0.0	0.0	-0.224
2500	0.1	0.1	0.1	0.1	0.1	0.0	0.0	0.0	0.0	0.0	-0.350
3000	0.1	0.1	0.1	0.1	0.1	0.1	0.1	0.1	0.0	0.0	-0.504
3500	0.1	0.1	0.1	0.1	0.1	0.1	0.1	0.1	0.1	0.1	-0.686
4000	0.1	0.1	0.1	0.1	0.1	0.1	0.1	0.1	0.1	0.1	-0.895
4500	0.1	0.1	0.1	0.1	0.1	0.1	0.1	0.1	0.1	0.1	-1.133
5000	0.1	0.1	0.1	0.1	0.1	0.1	0.1	0.1	0.1	0.1	-1.399
5500	0.2	0.1	0.1	0.1	0.1	0.1	0.1	0.1	0.1	0.1	-1.693
6000	0.2	0.2	0.1	0.1	0.1	0.1	0.1	0.1	0.1	0.1	-2.015
6500	0.2	0.2	0.2	0.1	0.1	0.1	0.1	0.1	0.1	0.1	-2.365
7000	0.2	0.2	0.2	0.2	0.1	0.1	0.1	0.1	0.1	0.1	-2.742
7500	0.2	0.2	0.2	0.2	0.2	0.1	0.1	0.1	0.1	0.1	-3.148
8000	0.2	0.2	0.2	0.2	0.2	0.2	0.1	0.1	0.1	0.1	-3.582
8500	0.2	0.2	0.2	0.2	0.2	0.2	0.2	0.1	0.1	0.1	-4.043
9000	0.2	0.2	0.2	0.2	0.2	0.2	0.2	0.2	0.1	0.1	-4.533

value as that of a plane circular plate for the radius of 1°. The potential change of a spherical Bouguer plate however is less negative with the increase of radius ψ . The value becomes zero around ψ = 39° , and beyond this point, the potential change is positive. As an example, Figure 9 shows the potential changes of the plate 3000 m high with respect to radius ψ computed from equations (36) and (40) for a spherical Bouguer plate, equations (41) and (43) for a plane circular plate and equation (44) for an infinite plane plate. Also shown in the Figure 9 is the difference of potential changes between the spherical Bouguer plate and the plane circular plate. The difference shows almost a linear function of radius ψ .

Comparing the potential of a spherical Bouguer plate computed from trigonometric functions (equation (36)) and that from hyperbolic functions by equation (38), it is found that both equations give the same numerical value up to 10^{-6}kgal-meter.

The computation of the potential change of the irregular part of topography, $\delta V''$ by equation (56) with equations (49) to (51) shows that V_4 term has a very small contribution to $\delta V''$. For example, using the cylindrical ring explained in Section 2.3 with radii between 1° to 2° and height 6000 m, the contribution of V_4 term is just 10^{-6} of $\delta V''$. The contribution of V_4 relative to $\delta V''$ is even smaller when the radii of the ring are large and/or the height is lower. Therefore, in most cases we do not need to use V_4 term in the computation of $\delta V''$.

Comparing Two Different Spherical Bouguer Plate (TDSBP) method, Two Different Plane Circular Plate (TDPCP) method and the integration method for determining the potential change at point P_o on the geoid of the ring of width 1° (the difference between angular radii ψ_1 and ψ_2 or their equivalent linear radii a_1 and a_2), a good agreement was found between TDPCP method and the integration method. This means that the expressions for potential change of a plane circular plate (equations (41) and (43)) is compatible with that of irregular part of

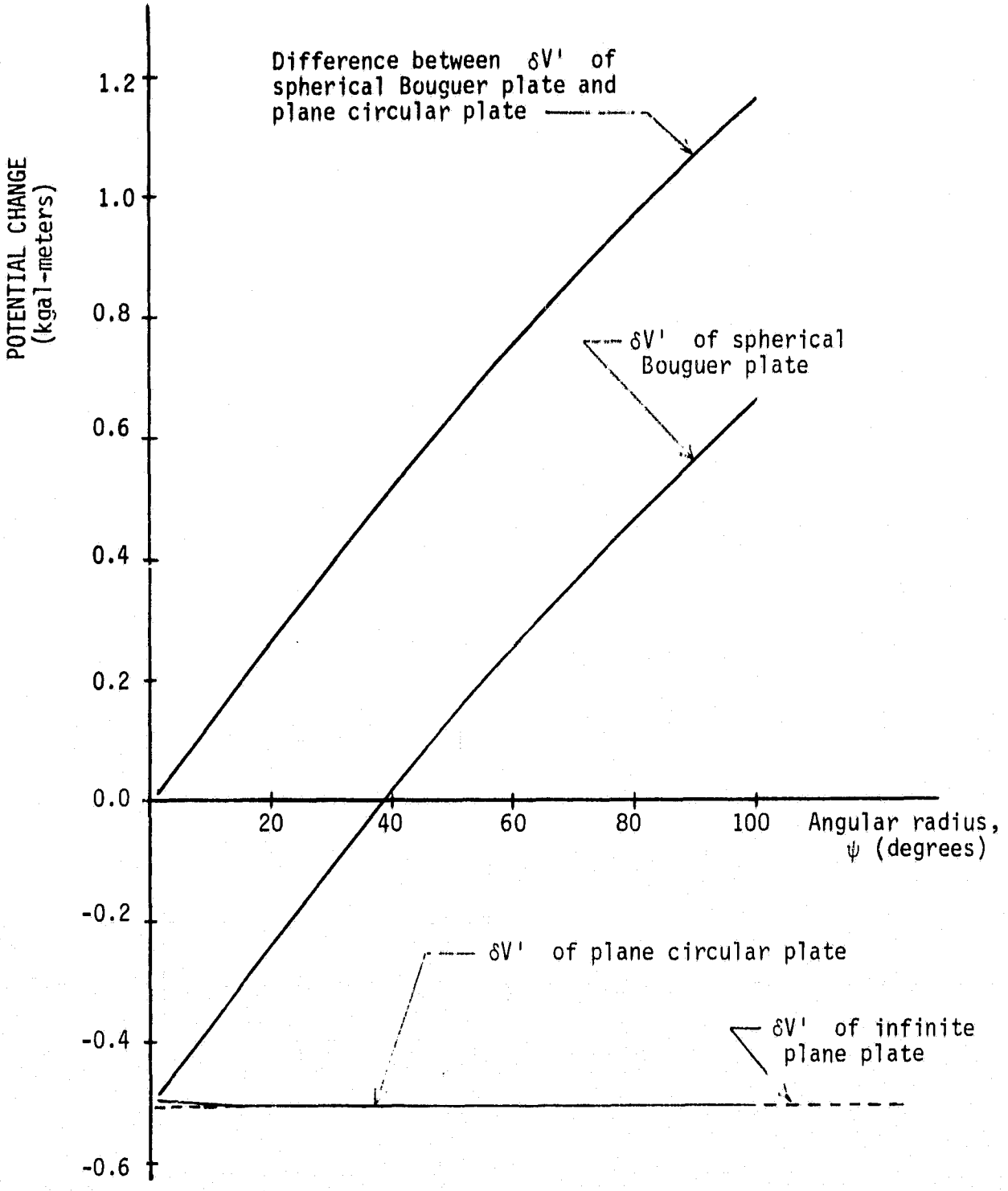

Figure 9: Potential changes of the regular part from different expressions for a spherical Bouguer plate, a plane circular plate and an infinite plane plate.

topography (equation (56)). Table 5 is the example showing the comparison TDPCP and integration method for the height of 3000 m. The discrepancy is less than 10^{-9} kgal-meters which is negligile.

2.3.2 Comparison of Formulas for Attraction Change

The attraction change in the second method of Helmert's condensation is the difference between the vertical attractions of the topography before the condensation and the condensed layer, evaluated at point P on the earth's surface. The attraction change is subtracted from the free-air anomaly to obtain the Helmert's anomaly. Table 6 and Table 7 show the attraction changes at point P on the surface when the topography is represented by the spherical Bouguer plate (SBP) using equations (61) and (63) and the plane circular plate (PCP) using equations (65) and (66). Height h_p of the plates varies from 500 m to 9000 m and spherical radius, ψ, varies from 1° to 20°. Comparing the values of the attraction changes of SBP and PCP for small plate (say $\psi \leq 10°$) reveals that the attraction change of SBP is about three times larger than that of PCP.

The attraction change of PCP becomes smaller as the radius of the plate increases and vanishes when the radius is infinitely large as we have proved in subsection 2.2.1(c). The attraction change of SBP computed from equations (61) and (63) however does not go to zero when $\psi = 180°$ or when the plate becomes the whole spherical shell. The expected value of a spherical shell at the point P is expected to be zero (see Table 1 on p. 16). Figure 10 shows the behavior of the attraction change of SBP with height 3000 m as the spherical angle increases from 10° to 180°. The minimum value of the attraction change occurs approximatley at $\psi = 70°$. This minimum point is compatible with the curve of the potential change of SBP plotted in Figure 9 where the maximum slope of the curve is also approximately at $\psi = 70°$. This is true regardless of the evaluation points for the potential change and the attraction change not being the same.

Table 5: Comparison of the potential change of a cylindrical ring 3,000 m high between Two Different Plane Circular Plate (TDPCP) method and integration method. ψ_1 is the inner radius of ring and a_1 is its corresponding linear distance taking R = 6371000 meter. $\delta V'$ is the potential change computed by the expressions for the plane circular plate and $\delta V''$ is that for the irregular part of topography.

ψ_1 (deg.)	a_1 (m)	$\delta V''$ (kgal-m)	$\delta V'$ (kgal-m)	$\delta V'' - \delta V'$ (kgal-m)
1	111194.	0.22643873D-02	0.22643873D-02	-0.11863340D-12
2	222379.	0.75485015D-03	0.75485015D-03	-0.10252112D-11
3	333547.	0.37741148D-03	0.37741148D-03	0.12346612D-12
4	444699.	0.22642645D-03	0.22642645D-03	0.50109172D-13
5	555798.	0.15093262D-03	0.15093262D-03	0.12192436D-13
6	666865.	0.10779290D-03	0.10779291D-03	-0.50216670D-11
7	777880.	0.80830425D-04	0.80830421D-04	0.37997591D-11
8	888837.	0.62855371D-04	0.62855378D-04	-0.64753843D-11
9	999726.	0.50272794D-04	0.50272803D-04	-0.82917451D-11
10	1110538.	0.41121805D-04	0.41121785D-04	0.19760230D-10
11	1221267.	0.34258543D-04	0.34258558D-04	-0.15054189D-10
12	1331902.	0.28979096D-04	0.28979090D-04	0.61158099D-11
13	1442435.	0.24830945D-04	0.24830971D-04	-0.26536668D-10
14	1552859.	0.21512411D-04	0.21512390D-04	0.21347645D-10
15	1663165.	0.18816090D-04	0.18816105D-04	-0.14529216D-10
16	1773344.	0.16595578D-04	0.16595573D-04	0.58858269D-11
17	1883388.	0.14745140D-04	0.14745140D-04	-0.11847763D-12
18	1993288.	0.13186864D-04	0.13186872D-04	-0.79439266D-11
19	2103037.	0.11862316D-04	0.11862334D-04	-0.16269318D-10

Table 6: Attraction change due to condensation when the topography is represented by a spherical Bouguer plate (in mgal) as computed from equations (61) and (63).

HEIGHT	ANGULAR RADIUS OF THE PLATE (DEGREES)																			
(M.)	1	2	3	4	5	6	7	8	9	10	11	12	13	14	15	16	17	18	19	20
500	0.4	0.2	0.1	0.1	0.1	0.1	0.1	0.1	0.1	0.1	0.0	0.0	0.0	0.0	0.0	0.0	0.0	0.0	0.0	0.0
1000	1.6	0.8	0.6	0.4	0.4	0.3	0.3	0.2	0.2	0.2	0.2	0.2	0.2	0.2	0.2	0.2	0.1	0.1	0.1	0.1
1500	3.5	1.8	1.3	1.0	0.8	0.7	0.6	0.5	0.5	0.5	0.4	0.4	0.4	0.4	0.4	0.3	0.3	0.3	0.3	0.3
2000	6.2	3.2	2.2	1.7	1.4	1.2	1.1	1.0	0.9	0.8	0.8	0.7	0.7	0.7	0.6	0.6	0.6	0.6	0.6	0.5
2500	9.8	5.0	3.5	2.7	2.2	1.9	1.7	1.5	1.4	1.3	1.2	1.1	1.1	1.0	1.0	1.0	0.9	0.9	0.9	0.8
3000	14.1	7.3	5.0	3.9	3.2	2.8	2.4	2.2	2.0	1.9	1.7	1.6	1.6	1.5	1.4	1.4	1.3	1.3	1.3	1.2
3500	19.1	9.9	6.8	5.3	4.4	3.8	3.3	3.0	2.7	2.5	2.4	2.2	2.1	2.0	1.9	1.9	1.8	1.8	1.7	1.7
4000	25.0	12.9	8.9	6.9	5.7	4.9	4.3	3.9	3.6	3.3	3.1	2.9	2.8	2.6	2.5	2.4	2.4	2.3	2.2	2.2
4500	31.6	16.4	11.3	8.7	7.2	6.2	5.5	4.9	4.5	4.2	3.9	3.7	3.5	3.4	3.2	3.1	3.0	2.9	2.8	2.7
5000	39.0	20.2	13.9	10.8	8.9	7.7	6.8	6.1	5.6	5.2	4.8	4.6	4.3	4.1	4.0	3.8	3.7	3.6	3.5	3.4
5500	47.2	24.4	16.8	13.0	10.8	9.3	8.2	7.4	6.8	6.3	5.9	5.5	5.2	5.0	4.8	4.6	4.5	4.3	4.2	4.1
6000	56.1	29.1	20.0	15.5	12.8	11.0	9.7	8.8	8.0	7.5	7.0	6.6	6.2	6.0	5.7	5.5	5.3	5.1	5.0	4.9
6500	65.9	34.1	23.5	18.2	15.0	12.9	11.4	10.3	9.4	8.7	8.2	7.7	7.3	7.0	6.7	6.5	6.2	6.0	5.9	5.7
7000	76.4	39.5	27.3	21.1	17.4	15.0	13.3	12.0	10.9	10.1	9.5	9.0	8.5	8.1	7.8	7.5	7.2	7.0	6.8	6.6
7500	87.6	45.4	31.3	24.2	20.0	17.2	15.2	13.7	12.6	11.6	10.9	10.3	9.8	9.3	8.9	8.6	8.3	8.0	7.8	7.6
8000	99.7	51.6	35.6	27.6	22.8	19.6	17.3	15.6	14.3	13.3	12.4	11.7	11.1	10.6	10.2	9.8	9.4	9.1	8.9	8.7
8500	112.5	58.3	40.2	31.1	25.7	22.1	19.5	17.6	16.1	15.0	14.0	13.2	12.5	12.0	11.5	11.0	10.7	10.3	10.0	9.8
9000	126.1	65.3	45.0	34.9	28.8	24.8	21.9	19.8	18.1	16.8	15.7	14.8	14.0	13.4	12.8	12.4	11.9	11.6	11.2	11.0

Table 7: Attraction change due to condensation when the topography is represented by a plane circular plate (in mgal) as computed from equations (65) and (66).

HEIGHT	EQUIVALENT ANGULAR RADIUS OF THE PLATE (DEGREES)																			
(M.)	1	2	3	4	5	6	7	8	9	10	11	12	13	14	15	16	17	18	19	20
500	0.1	0.1	0.0	0.0	0.0	0.0	0.0	0.0	0.0	0.0	0.0	0.0	0.0	0.0	0.0	0.0	0.0	0.0	0.0	0.0
1000	0.5	0.3	0.2	0.1	0.1	0.1	0.1	0.1	0.1	0.1	0.0	0.0	0.0	0.0	0.0	0.0	0.0	0.0	0.0	0.0
1500	1.1	0.6	0.4	0.3	0.2	0.2	0.2	0.1	0.1	0.1	0.1	0.1	0.1	0.1	0.1	0.1	0.1	0.1	0.1	0.1
2000	2.0	1.0	0.7	0.5	0.4	0.3	0.3	0.3	0.2	0.2	0.2	0.2	0.2	0.1	0.1	0.1	0.1	0.1	0.1	0.1
2500	3.1	1.6	1.0	0.8	0.6	0.5	0.4	0.4	0.3	0.3	0.3	0.3	0.2	0.2	0.2	0.2	0.2	0.2	0.2	0.2
3000	4.5	2.3	1.5	1.1	0.9	0.8	0.6	0.6	0.5	0.5	0.4	0.4	0.3	0.3	0.3	0.3	0.3	0.3	0.2	0.2
3500	6.2	3.1	2.1	1.5	1.2	1.0	0.9	0.8	0.7	0.6	0.6	0.5	0.5	0.4	0.4	0.4	0.4	0.3	0.3	0.3
4000	8.0	4.0	2.7	2.0	1.6	1.3	1.2	1.0	0.9	0.8	0.7	0.7	0.6	0.6	0.5	0.5	0.5	0.4	0.4	0.4
4500	10.2	5.1	3.4	2.5	2.0	1.7	1.5	1.3	1.1	1.0	0.9	0.9	0.8	0.7	0.7	0.6	0.6	0.6	0.5	0.5
5000	12.6	6.3	4.2	3.1	2.5	2.1	1.8	1.6	1.4	1.3	1.1	1.1	1.0	0.9	0.8	0.8	0.7	0.7	0.7	0.6
5500	15.2	7.6	5.1	3.8	3.0	2.5	2.2	1.9	1.7	1.5	1.4	1.3	1.2	1.1	1.0	1.0	0.9	0.8	0.8	0.8
6000	18.1	9.1	6.0	4.5	3.6	3.0	2.6	2.3	2.0	1.8	1.6	1.5	1.4	1.3	1.2	1.1	1.1	1.0	1.0	0.9
6500	21.2	10.6	7.1	5.3	4.3	3.5	3.0	2.7	2.4	2.1	1.9	1.8	1.6	1.5	1.4	1.3	1.3	1.2	1.1	1.1
7000	24.6	12.3	8.2	6.2	4.9	4.1	3.5	3.1	2.7	2.5	2.2	2.1	1.9	1.8	1.6	1.5	1.5	1.4	1.3	1.2
7500	28.2	14.1	9.4	7.1	5.7	4.7	4.0	3.5	3.1	2.8	2.6	2.4	2.2	2.0	1.9	1.8	1.7	1.6	1.5	1.4
8000	32.1	16.1	10.7	8.1	6.4	5.4	4.6	4.0	3.6	3.2	2.9	2.7	2.5	2.3	2.2	2.0	1.9	1.8	1.7	1.6
8500	36.2	18.2	12.1	9.1	7.3	6.1	5.2	4.5	4.0	3.6	3.3	3.0	2.8	2.6	2.4	2.3	2.1	2.0	1.9	1.8
9000	40.6	20.4	13.6	10.2	8.2	6.8	5.8	5.1	4.5	4.1	3.7	3.4	3.1	2.9	2.7	2.6	2.4	2.3	2.2	2.0

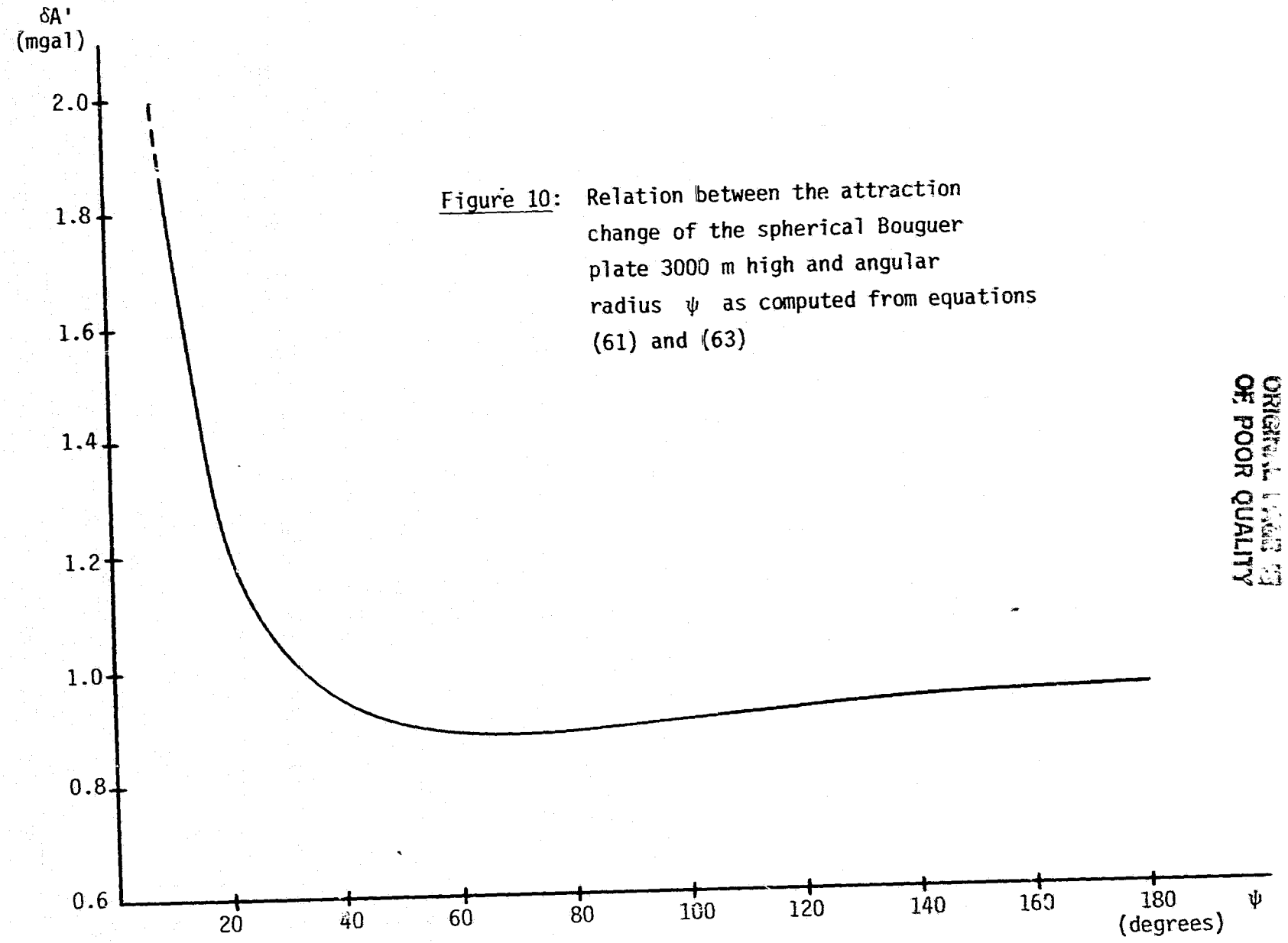

Figure 10: Relation between the attraction change of the spherical Bouguer plate 3000 m high and angular radius ψ as computed from equations (61) and (63)

Table 8: Comparison of the attraction change of a cylindrical ring 3,000 m high between Two Different Plane Circular Plate (TDPCP) method and integration method. ψ_1 is the inner radius of ring and a_1 is its corresponding linear distance taking R = 6371000 meter. $\delta A'$ is the attraction change computed by the expressions for the plane circular plate and $\delta A''$ is that for the irreglar part of topography.

ψ_1 (deg.)	a_1 (m)	$\delta A''$ (mgal)	$\delta A'$ (mgal)	$\delta A'' - \delta A'$ (mgal)
1	111194.	0.22648290D-02	0.22626576D-02	0.21623922D-05
2	222379.	0.75490166D-03	0.75468416D-03	0.21749959D-06
3	333547.	0.37742207D-03	0.37736911D-03	0.52953204D-07
4	444689.	0.22643022D-03	0.22641136D-03	0.18859667D-07
5	555793.	0.15093429D-03	0.15092595D-03	0.83374767D-08
6	666865.	0.10779375D-03	0.10778951D-03	0.42411458D-08
7	777880.	0.80830901D-04	0.80828520D-04	0.23813839D-08
8	888837.	0.62855659D-04	0.62854220D-04	0.14389949D-08
9	999726.	0.50272979D-04	0.50272058D-04	0.92033098D-09
10	1110538.	0.41121928D-04	0.41121312D-04	0.61583303D-09
11	1221267.	0.34258629D-04	0.34258201D-04	0.42754606D-09
12	1331902.	0.28979157D-04	0.28978851D-04	0.30608295D-09
13	1442435.	0.24830990D-04	0.24830765D-04	0.22491537D-09
14	1552859.	0.21512445D-04	0.21512276D-04	0.16892510D-09
15	1663165.	0.18816116D-04	0.18815987D-04	0.12937336D-09
16	1773344.	0.16595599D-04	0.16595498D-04	0.10072889D-09
17	1883388.	0.14745156D-04	0.14745076D-04	0.79625104D-10
18	1993288.	0.13186877D-04	0.13186813D-04	0.63760583D-10
19	2103037.	0.11862329D-04	0.11862277D-04	0.51676748D-10

It should be noted that the value of attraction change of the spherical Bouguer plate (SBP) at $\psi = 180°$ used in Figure 10 was computed by using $\psi = 179.99$ degrees. The attraction change of SBP for ψ being exactly 180° is indeterminate. We can see this by examining equation (62) that we get $\sinh\phi = \frac{0}{0}$ which is not defined when $\psi = 180°$. This is why we have taken the limiting value when $\psi \to 180°$.

The attraction expressions of the regular and irregular parts of the topography are compared by using the rings of the same mass in TDSBP, TDPCP and the integration methods. It is found that there is a good agreement between the expressions of PCP (equations (65) and (66)) and the expression of the irregular part (equation (69) with (68)). Table 8 is an example for the cylindrical ring 3000 m high. The discrepancy between the attraction changes from the two methods is less than 10^{-5} mgal at $\psi = 1°$ and it becomes even smaller when ψ increases.

2.3.3 Conclusion and Discussion

At the first glance we would say that the expressions for spherical Bouguer plate should give a more accurate result than those for the plane circular plate since the spherical plate better approximates the earth than does the plane plate. However, after examining the numerical results, the expressions for the spherical plate may not be appropriate. If we look at Figure 9, we see that the potential change at the point P_0 of the spherical Bouguer plate is increasing while the angular radius of the plate is increasing and it would be a positive value for the whole spherical shell ($\psi = 180°$). Comparing this to the value from Table 1, the potential change at the point P_0 of the spherical shell is negative. Moreover, the attraction change at the point P of a spherical Bouguer plate is not zero when $\psi = 180°$ (see for example Figure 10). This result contradicts the attraction change at the point P of the spherical shell shown in Table 1. This means that the expressions of potentials and attractions that we have for the spherical Bouguer plate (equations (36) to (40) and (61) to (64)) do not reflect the reality when $\psi = 180°$. So there must be some limitations to these expressions.

We consider now the expressions for a plane circular plate. As the radius of the plane circular plate increases, the value of potential change at the point P_0 computed from equations (41) and (43) goes toward the potential change of the infinite plane plate. The value of attraction change at point P computed from equations (65) and (66) goes toward zero which is the value of the attraction change of the infinite plane plate.

Although the potential change due to condensation at the point P_0 of the infinite plane plate is not significantly different from that of the plane circular plate, the attraction change at point P on the earth's surface of the infinite plane plate is. For example, the difference in attraction change between the two models is 0.9 mgals for the plate of 3000 m height and $\psi = 5°$. This magnitude of the attraction change difference gives significant effect on the geoid computation.

When we compared the expressions for potentials and attractions of the regular part of topography with those of the irregular part using TDSBP, TDPCP and integration methods (explained at the beginning of Section 2.3), we found that the expressions of the plane circular plate give a good agreement both in potential change and attraction change with those of the irregular part.

We see that the potential change and attraction change of the plane circular plate can be compensated by those of the irregular part. When the plane circular plate is extended, its expressions for potentials and attractions reflect the correct values. Based on these reasons, the plane circular plate will be used to represent the regular part of topography in the next chapter.

In chapter 3, we will develop procedures to compute the potential change and the attraction change due to Helmelt's condensation using $1° \times 1°$ mean elevations.

3. Calculation of the Indirect Effects and the Attraction Change Effect Using 1°x1° Mean Elevation Data

We have seen from equation (11) in Chapter 1 that to compute an accurate geoid, we must take into acount (i) the indirect effect, δN on geoid undulation due to the potential change in the second method of Helmert's condensation, δV discussed in Section 2.1; (ii) the effect of attraction change in gravity reduction which is equal to the terrain correction, C for planar approximation plus a small value of the attraction change of the regular part depending on the cap size used in computaion; and probably (iii) the secondary indirect effect on gravity, δ .

Before we develop a procedure to compute these corrections on the global basis, using information of 1°x1° mean elevations we should know how geoid undulations are practically computed so that, if possible, we can incorporate or apply the corrections properly.

3.1 Computational Methods for Geoid Undulations

Stokes' equation in the form of equation (1) cannot be used directly in practice because the information on gravity anomalies at every point on the earth is not available and the computation on the global basis requires a lot of computational effort. Two basic methods are discussed by Rapp and Rummel (1975) as follows:

Method 1: the geoid undulation;

$$N_1 = N_0 + \frac{R}{4\pi\gamma} \iint_{\sigma_c} S(\psi)\,(\Delta g_I - \Delta g_{ref})\, d\sigma_c + N_{ref} \qquad (74)$$

where the integral of the second term on the right-hand side is extended over cap size σ_c and the zero order undulation,

$$N_0 = -\frac{R}{2\gamma}\,\Delta g_0 + \frac{k\,\delta M}{2\gamma R} \qquad (75)$$

$$N_{ref} = R \sum_{n=2}^{\bar{n}} \sum_{m=0}^{n} (\bar{C}^{*}_{nm} \cos m\lambda + \bar{S}_{nm} \sin m\lambda)\, \bar{P}_{nm}(\sin\bar{\phi}) \tag{76}$$

and

$$\Delta g_{ref} = \gamma \sum_{n=2}^{\bar{n}} (n-1) \sum_{m=0}^{n} (\bar{C}^{*}_{nm} \cos m\lambda + \bar{S}_{nm} \sin m\lambda)\, \bar{P}_{nm}(\sin\bar{\phi}) \tag{77}$$

In this method, N_{ref} is the geoid undulation computed from fully normalized geopotential coefficients $\bar{C}^{*}_{nm}$ and $\bar{S}_{nm}$. The short wavelength part of the geoid is recovered by using gravity anomalies Δg_I with the cap size σ_c.

Method 2: the geoid undulation is computed from gravity anomalies in a certain cap size σ_c with Molodensky's truncation coefficients $Q_n(\psi)$ compensating for the effect of anomalies outside the cap. The basic equation is

$$N_1 = N_0 + \frac{R}{4\pi\gamma} \iint_{\sigma_c} S(\psi)\, \Delta g_I\, d\sigma_c + \frac{R}{2\gamma} \sum_{n=2}^{\infty} Q_n(\psi)\, \Delta g_n(\bar{\phi},\lambda) \tag{78}$$

where Δg_n is the degree anomaly computed from

$$\Delta g_n = \gamma(n-1) \sum_{m=0}^{n} (\bar{C}^{*}_{nm} \cos m\lambda + \bar{S}_{nm} \sin m\lambda)\, \bar{P}_{nm}(\sin\bar{\phi}) \tag{79}$$

When equations (74) and (78) are used, the integration over the infinitely small area $d\sigma_c$ is replaced by the summation over a certain finite area, e.g., $1°\times 1°$ area, then Δg_I are mean anomalies over the area.

In the next section, we consider how to compute indirect effect due to potential change from $1°\times 1°$ mean elevations.

3.2 Indirect Effect Due to Potential Change

The total potential change, at point P_0 on the geoid, δV, caused by the second method of Helmert's condensation, can be computed in two parts. One belongs to the regular part of topography and the other belongs to the irregular part or the topographic variation. Once the cap size ψ is chosen,

the potential change at the point P_0 of the former part is a straight forward computation (see Subsection 2.1.1, page 21). The potential change at the point P_0 of the irregular part is computed by summing up V_2, V_3, etc. terms (See Equations (56) and (49) to (51)). Since these V_i terms are in the integral forms which use the continuous function of topographic heights, we must modify them to suit the computation which uses the discrete mean heights of the block. Now consider the V_2 term from equation (49),

$$V_2 = -\frac{1}{6} k\rho R^2 \iint_\sigma \frac{h^3 - h_p^3}{\ell_0^3} d\sigma$$

Let dS represent the surface area of a sphere of radius R then,

$$dS = R^2 d\sigma \tag{80}$$

So we can write

$$V_2 = -\frac{1}{6} k\rho \iint_S \frac{h^3 - h_p^3}{\ell_0^3} dS \tag{81}$$

In practice, we have to represent the infinitely small area dS by some finite area ΔA_i and we can substitute the integration by a summation. Therefore

$$V_2 = -\frac{1}{6} k\rho \sum_{i=1}^{m} \frac{h_i^3 - h_p^3}{\ell_{0i}^3} \cdot \Delta A_i \tag{82}$$

where m = number of ΔA_i on the surface S

h_i = average height over an area ΔA_i

ℓ_{0i} = distance from the computation point P_0 to the center of the small area ΔA_i .

In the same way, the other terms from equation (50) and (51) can be written as

$$V_3 = \frac{3}{40} k\rho \sum_{i=1}^{m} \frac{h_i^5 - h_p^5}{\ell_{0i}^5} \cdot \Delta A_i$$

$$V_4 = -\frac{15}{336} k\rho \sum_{i=1}^{m} \frac{h_i^7 - h_p^7}{\ell_{0i}^7} \cdot \Delta A_i \tag{83}$$

Up to this point we separate the computation of the potential change of the irregular part of topography from that of the regular part. However, we have seen from Chapter 2 that if the regular part is represented by a plane circular plate, we can then get the same potential change of the plate by using the expressions for the potential change of the irregular part of topography. This means that instead of using the expression for a plane circular plate: (i) we can break the plane circular plate into pieces such as consecutive series of cylindrical rings; (ii) use the expression for irregular part to compute the effect of an individual piece; (iii) sum them up and we still get the same result.

We are now going to show that by applying the above idea with 1°x 1° mean height information, we can combine the potential change of the regular part with that of the irregular part. Instead of breaking the topographic masses into pieces of cylindrical rings, we break them into prisms of masses above 1°x 1° areas, i.e., the topography of the earth consists of a series of rectangular columns. Now we can use equation (56) with equations (82) and (83) to compute the potential change of the plane circular plate where ΔA_i is the area of a 1°x 1° block. Taking the height of topography h_i in equations (82) and (83) to be h_p and the height of the reference surface, h_p in those equations to be zero, we obtain the components of the potential change of the plane circular plate to be:

$$V_2' = -\frac{1}{6}k\rho \sum_{i=1}^{m} \frac{h_p^3 - 0}{\ell_{0i}^3} \Delta A_i$$

$$V_3' = \frac{3}{40}k\rho \sum_{i=1}^{m} \frac{h_p^5 - 0}{\ell_{0i}^5} \Delta A_i \qquad (84)$$

$$V_4' = -\frac{15}{336}k\rho \sum_{i=1}^{m} \frac{h_p^7 - 0}{\ell_{0i}^7} \Delta A_i$$

We, now, combine the potential change of the regular part (equation (84)) and the irregular part (equation (82), (83)) algebraically. Then the individual component of the potential change can be computed from

$$V_2 = -\frac{1}{6}k\rho \sum_{i=1}^{m} \left(\frac{h_i}{\ell_{0i}}\right)^3 \cdot \Delta A_i$$

$$V_3 = \frac{3}{4\pi} k\rho \sum_{i=1}^{m} \left(\frac{h_i}{\ell_{0_i}}\right)^5 \cdot \Delta A_i \qquad (85)$$

$$V_4 = -\frac{15}{336} k\rho \sum_{i=1}^{m} \left(\frac{h_i}{\ell_{0_i}}\right)^7 \cdot \Delta A_i$$

That is the potential change at the point P_0 on the geoid of the topography

$$\delta V = V_2 + V_3 + V_4 + \ldots$$

$$= -k\rho \sum_{i=1}^{m} \Delta A_i \left\{ \frac{1}{6} \left(\frac{h_i}{\ell_{0_i}}\right)^3 - \frac{3}{40} \left(\frac{h_i}{\ell_{0_i}}\right)^5 \right.$$

$$\left. + \frac{15}{336} \left(\frac{h_i}{\ell_{0_i}}\right)^7 - \ldots \right\} \qquad (86)$$

We can see that the potential change affected by block i depends on two parameters h_i and ℓ_{0i}. This makes it easy to compute the potential change of the individual block. After summing up the effects of all blocks, the indirect effect due to potential change is found from Brun's formula of equation (4). This indirect effect represents the mean value at the center of the central block.

In this section, we have not addressed the problem of the central block, which is the block containing the computation point, where ℓ_0 is zero. This will be discussed in Section 3.5. Next, we consider how to compute the attraction change effect on geoid undulation from 1°x 1° mean heights.

3.3 Attraction Change Effect on Geoid Undulation

An attraction change effect on geoid undulation is an effect coming from the attraction change when the topographic masses are condensed in Helmert's condensation reduction. The total attraction change is the sum of the attraction changes of the regular and the irregular parts of the topography, i.e., $\delta A = \delta A' + \delta A''$. The attraction change of the regular part, $\delta A' = A' - A'_S$ is computed using equation (65) and (66), while the attraction change of the irregular part is equal to the terrain correction in the planar approximation. Similar to expressions for V_2, V_3, V_4, etc. in equations (82) and (83), the terrain correction can be written as

$$\delta A'' = \tfrac{1}{2} k\rho \sum_{i=1}^{m} \frac{(h_i - h_p)^2}{\ell^3_{\delta i}} \Delta A_i \qquad (87)$$

Unlike the effect of the potential changes, we cannot combine the effects of the attraction change of the regular part and the irregular part into one-step computation since the terrain correction is always positive whether or not the mass is above or below the surface of the plate. That is the more rugged the terrain is, the greater the attraction change is. The sum of $\delta A'$ and $\delta A''$ is assumed to be the average attraction change in the central $1° \times 1°$ block.

After the total attraction change has been computed, we can add it to the free air anomaly before using in Stokes' equation (see equation (9). Otherwise, we can compute the correction due to attraction change separately (see equation (10)) if the geoid undulation was already computed with uncorrected anomalies.

In order to compute the attraction change effect on geoid undulation separately, we must know how the geoid undulations in the area of interest were obtained. For example, if Method 1 of Section 3.1 is used to compute the geoid undulation from free-air anomalies and the geopotential coefficients derived from satellite altimeter. The satellite derived undulations are not affected by the topographic masses above the geoid. This means that no topographic corrections are needed for the information outside cap size σ_c. Therefore, the cap size used for computing the attraction change effect on geoid undulation should be the same as that used in the computation of geoid undulation. There are two ways which we can use to compute the attraction change effect on geoid undulation from the $1° \times 1°$ mean attraction change that we have.

Method A: Use the direct Stokes' equation for the attraction change within cap size σ_c. The effect of the attraction change on geoid undulation is then:

$$\Delta N_1 = \frac{R}{4\pi\gamma} \iint_{\sigma_c} \delta A \, S(\psi) \, d\sigma \qquad (88)$$

Method B: Use $1° \times 1°$ attraction changes over the whole world to develop correction terms to potential coefficients of the attraction change

field using the programs for harmonic development by Colombo (1981), (or programs of a similar nature). These correction terms are then used to compute the undulation change. The equation for computing the undulation change within the cap size σ_c is modified from equation (51) of Rapp (1981) to include the zeroth- and the first-degree components of the attraction changes. This equation is:

$$\Delta N_1 = \frac{R}{2\gamma} \sum_{n=2}^{\bar{n}} (2-Q_n(n-1))\ \delta A_n + \frac{R}{2\gamma} \sum_{n=0}^{1} Q_n\ \delta \bar{A}_n \qquad (89)$$

where

$$\delta A_n = \sum_{m=0}^{n} (\delta C_{nm} \cos m\lambda + \delta S_{nm} \sin m\lambda)\ P_{nm}(\sin\bar{\phi}) \qquad (90)$$

$$\delta \bar{A}_n = \sum_{m=0}^{n} (\delta C_{nm}^{(\Delta g)} \cos m\lambda + \delta S_{nm}^{(\Delta g)} \sin m\lambda)\ P_{nm}(\sin\bar{\phi})$$

δC_{nm} and δS_{nm} in equation (90) are corrections in terms of the potential coefficients. $\delta C_{nm}^{(\Delta g)}$ and $\delta S_{nm}^{(\Delta g)}$ are corrections in terms of the anomaly coefficients. These coefficients are developed from the attraction changes due to the second method of Helmert's condensation. Q_n is the Molodensky's truncation coefficient of degree n which depends on cap size σ_c. $\bar{n}$ is the maximum degree of harmonic coefficients used for the computation. The derivation of equation (89) is shown in Appendix A.

3.4 Secondary Indirect Effect

After we have obtained the indirect effect due to the potential change in the 1°x1° block, we can use equation (5) to compute the secondary indirect effect on gravity, δ. The value δ is thus the mean value within the 1°x1° block too. We can add δ to $\Delta g + \delta A$ so that we compute the corrected geoid undulation. Otherwise, we can compute the correction term due to the secondary indirect effect on gravity separately in the same way we compute the attraction change effect on geoid undulation (see Section 3.3).

3.5 Problem of the Central Block

The central block is defined to be the smallest elevation block which contains the computation point P on the earth's surface or point P_0 on the geoid. From equations (86) and (87), we see that $\delta V''$ and $\delta A''$ vary with the inverses of $\ell_{0_i}^3$, $\ell_{0_i}^5$, etc. This means that $\delta V''$ and $\delta A''$ are influenced significantly by the information in the innermost zone around the computation point P_0 or P and they vanish when ℓ_{0_i} is very large. Consequently we should use more detailed information in the innermost zone. For example, if we are working with 1°x1° information then we might use 5'x5' mean elevations in the innermost zone. The size of the central block is then 5'x5'. We call the 1°x1° block which contains the computation points as the central zone. The other 1°x1° blocks within the cap size for computing the potential change and the attraction change are called blocks in the outer zone. The detailed information however helps to give a better value in computing $\delta A''$ only. The reason is that in computing $\delta V''$, if the value of 1°x1° mean elevation that we have represents the average elevation of all 5'x5' mean elevations in the same 1°x1° block, then both $\delta V''$ computed from either size of the mean elevation should be the same. It is not necessary then to use 5'x5' mean elevations for computing the potential change $\delta V''$. The attraction change $\delta A''$ of the central zone (1°x1° block) is zero if only one 1°x1° mean elevation is used. The change $\delta A''$ is not zero however if 5'x5' mean elevations in the central zone are used and at least one of them is different from the 1°x1° mean elevation of the corresponding block.

No matter what size of block are used in the calculation of $\delta V''$ and $\delta A''$ in the central zone, we have a problem with the central block or zone where ℓ_0 is zero and the effect of the topography is indeterminable. Therefore, we now consider how to handle the information of the central block. The potential change and the attraction change of the central block are computed as follows:

(a) To compute the potential change $\delta V''$, the central block is substituted by the plane circular plate having the same mass as the prism of masses above the central block. The following equation is used to obtain the radius of the equivalent plane circular plate:

Table 9: Postulated 1°x 1° Mean Terrain Corrections As a Function of the Block Elevation

Model 1		Model 2		Model 3	
Height*	Ter.Cor.	Height*	Ter.Cor.	Height*	Ter.Cor.
0 m	0 mgals	200 m	0 mgals	300 m	0 mgals
200	1	400	1	500	1
400	3	600	2	800	2
600	5	800	3	1000	3
800	6	1000	4	1500	4
1000	7	1200	5	2000	5
1500	8	1400	6	2500	6
2000	9	1600	7	3000	7
2500	10	1800	8	3500	8
3000	12	2000	9	4000	9
3500	14	2200	10	9000	10
4000	15	2400	11		
4500	17	2600	12		
5000	18	2800	13		
9000	20	3000	14		
		3200	15		
		3400	16		
		3600	17		
		3800	18		
		4000	20		
		9000	21		

*The terrain correction is given for an elevation between the specified elevation and the previous elevation. (For example, in model 1, if a 1°x 1° mean elevation fell between 1500 and 2000 m, the adopted terrain correction was 9 mgals). The terrain correction was zero for all oceanic blocks. (From Rapp, 1977).

$$\psi = 2 \sin^{-1}\left[\frac{\theta\ (\sin\phi_2 - \sin\phi_1)}{4\pi}\right]^{\frac{1}{2}}$$

where θ is the side of the equiangular block which is bounded by parallels ϕ_1 and ϕ_2. Both ψ and θ are in radians. Note that $(\sin\phi_2 - \sin\phi_1)$ can be approximately computed by $\cos\phi_1 \sin\theta$.

(b) The computation of the attraction change or the terrain correction of the central block requires a lot of data and efforts to obtain an accurate result. It can be computed by using detailed height information in a very small block (Dimitrijevich et al., 1976) or by least square collocation (Forsberg and Tscherning, 1981). However, the compuation of the terrain correction is not the main interest of this study, so we will use the postualted model given by Rapp (1977) to get the mean terrain correction of the 1°x1° block. The postulated models are shown in Table 9. The mean terrain correction given by these models include not only the effect of the topography in the central 1°x1° block but also the effect of the topography in the outer zone.

3.6 Summary of the Procedures and Equations for Computing an Accurate Geoid Using 1°x1° Mean Elevations

In this section we summarize the procedures and the important equations used for computing an accurate geoid discussed earlier in the previous sections.

The theoretically more accurate geoid is obtained if Helmert's anomalies are used in the Stokes' equation and the indirect effects are taken into account. The equation to compute a more accurate geoid undulation is:

$$N = N_1 + \Delta N_1 + \delta N_2 + \delta N \qquad (11)$$

N_1 is the free-air geoid undulation. The terms ΔN_1, δN_2 and δN are correction terms which can be calculated as follows:

(a) The potential change effect or the indirect effect, δN :

$$\delta N = \frac{\delta V}{\gamma} \qquad (3)$$

The potential change, δV is the difference between the potential of the topography and the potential of the condensed layer evaluated at point P_0 on the geoid. The effects of the regular and the irregular parts of the topography are combined into a one-step computation. A cap size ψ_1 is chosen for computing the potential change in such a way that the effect of the topographic masses outside this cap will be negligible. The potential change is the sum of the following two components.

1. The potential change of the central block is computed using:

$$\delta V = V' - V'_s$$

where

$$V' = \pi k\rho \left[-h_p^2 + h_p E_1 + a^2 \ell n \frac{h_p+E_1}{a}\right]; \quad E_1 = \sqrt{a^2+h_p^2} \tag{41}$$

$$V'_s = 4\pi k\rho\, h_p R \sin\frac{\psi}{2} \tag{43}$$

$$\psi = 2 \sin^{-1}\left[\frac{\theta(\sin\phi_2 - \sin\phi_1)}{4\pi}\right]^{\frac{1}{2}}$$

and

$$a = 2 R \sin\frac{\psi}{2} \tag{42}$$

θ is the side of the equiangular block which equals one degree in our case.

2. The potential change of the blocks in the outer zone is computed from

$$\delta V = -k\rho \sum_{i=1}^{m} \Delta A_i \left\{ \tfrac{1}{6}\left(\frac{h_i}{\ell_{0_i}}\right)^3 - \tfrac{3}{40}\left(\frac{h_i}{\ell_{0_i}}\right)^5 + \ldots\right\} \tag{86}$$

(b) The attraction change effect on geoid undulation, ΔN_1 .

We can use either the Stokes' equation:

$$\Delta N_1 = \frac{R}{4\pi\gamma} \iint_{\sigma_c} \delta A\, S(\psi)\, d\sigma \tag{88}$$

or the harmonic series:

$$\Delta N_1 = \frac{R}{2} \sum_{n=2}^{\bar{n}} (2 - Q_n(n-1))\, \delta A_n + \frac{R}{2\gamma} \sum_{n=0}^{1} Q_n\, \delta \bar{A}_n \tag{89}$$

where

$$\delta A_n = \sum_{m=0}^{n} (\delta C_{nm} \cos m\lambda + \delta S_{nm} \sin m\lambda) P_{nm}(\sin\phi)$$

$$\delta \bar{A}_n = \sum_{m=0}^{n} (\delta C_{nm}^{(\Delta g)} \cos m\lambda + \delta S_{nm}^{(\Delta g)} \sin m\lambda) P_{nm}(\sin\phi) \qquad (90)$$

The attraction change is the difference between the vertical attraction of the topography and the vertical attraction of the condensed layer evaluated at point P on the earth's surface. A cap size ψ_2 is selected for computing the attraction change. It may be the same as the cap ψ_1 depending on how accurate the value of the change required. Using a larger cap size yields a more accurate result since information in the larger area is taken into account. The attraction change consists of the effects of the regular and irregular parts of the topography.

1. The attraction change of the regular part of the topography within the cap size ψ_2 (or the corresponding linear radius a) is computed from:

$$\delta A' = A' - A'_s$$

where

$$A' = 2\pi k\rho \left(a + h_p - \sqrt{a^2+h_p^2}\right) \qquad (65)$$

$$A'_s = 2\pi k\rho h_p \left(1 - \frac{h_p}{\sqrt{a^2+h_p^2}}\right) \qquad (66)$$

2. The attraction change of the irregular part of the topography or the terrain correction is computed from:

$$\delta A'' = \tfrac{1}{2} k\rho \sum_{i=1}^{m} \frac{(h_i - h_p)^2}{\ell^3_{0i}} \Delta A_i \qquad (87)$$

Rapp's postulated model 1 given in Table 9, however, will be used to obtain the terrain correction in this study.

(c) The secondary indirect effect on geoid undulation, δN_2 :

$$\delta N_2 = \frac{R}{4\pi\gamma} \iint_{\sigma_c} \delta S(\psi)\, d\sigma$$

where the secondary indirect effect on gravity, δ is obtained from

$$\delta = 0.3086\ \delta N \qquad (5)$$

In the next chapter, we present the results of indirect effects due to the potential changes, attraction change effects on geoid undulation and the secondary indirect effects in the test area using procedures explained in this section.

4. Results in the Test Area

An area referred to as an output area, which is used to test the previous ideas, was selected to extend from latitude 20°N to latitude 50°N and from longitude 130°W to 65°W. A data area where mean elevations of 1°x 1° equiangular blocks were used to compute the potential and attraction changes, then, has to be larger than 30° x 65°. It depends separately on the cap sizes sizes that we use to compute the changes and the cap size σ_c in Stokes' equation. For example, Figure 11 is the diagram showing the data area of 1°x 1° mean elevations needed to get attraction change effects on geoid undulation in the output area of 30° x 65° when the 10° cap is used in Stokes' equation and the 5° cap is used to compute the attraction changes. The effect of the potential change on the geoid undulation is computed directly from the the indirect effects due to potential change within the same output area is smaller. Figure 12 is the contour map showing topographic heights above the geoid in the output area.

In the next section, we look at the effects of the potential changes due to Helmert's condensation in the test area.

4.1 Effect of Potential Changes on Geoid Undulations

The indirect effect due to the potential change in the second method of Helmert's Condensation was computed by the procedure explained in section

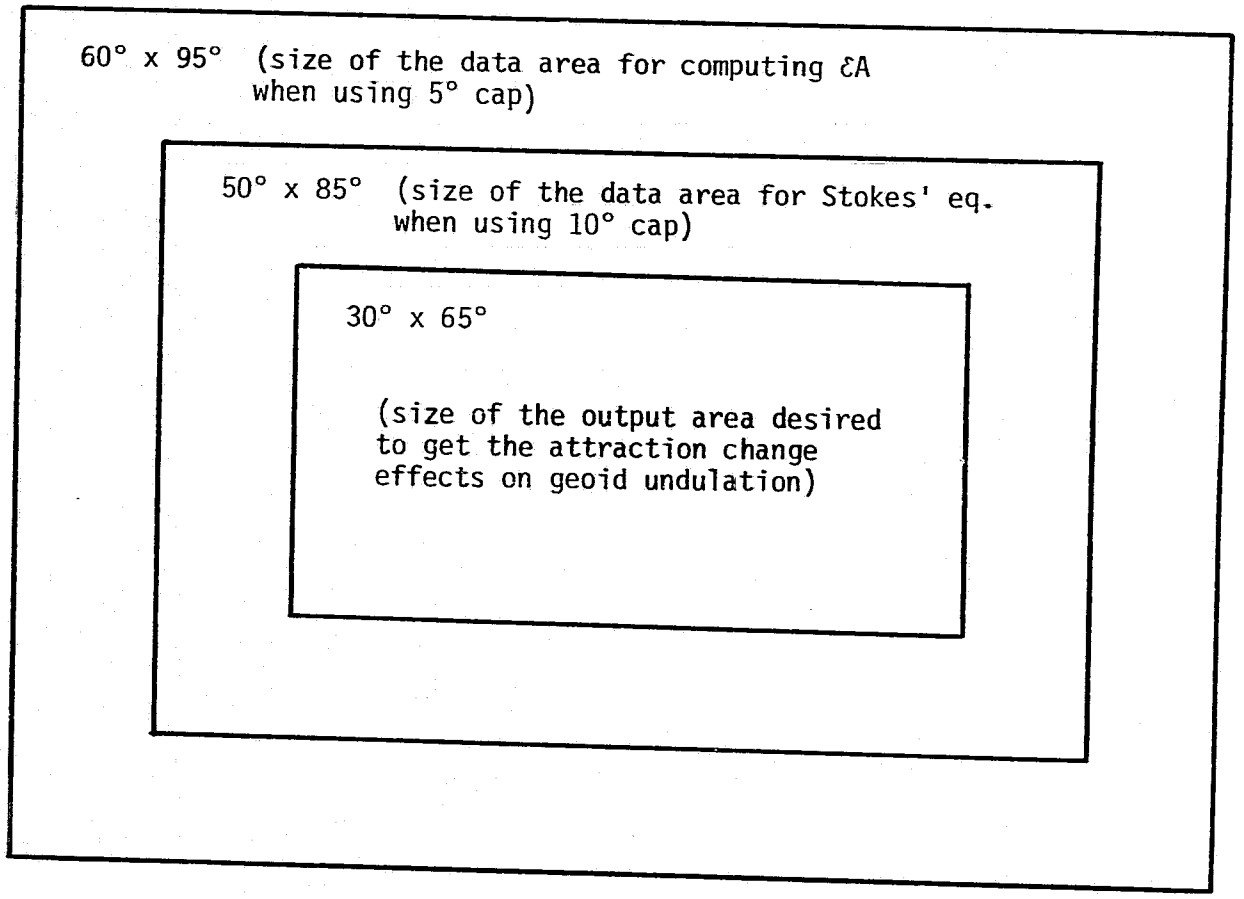

Figure 11: A diagram showing the sizes of area needed to get the attraction change effects on geoid undulation when 10° cap is used in Stokes' equation and 5° cap is used in computing the attraction change.

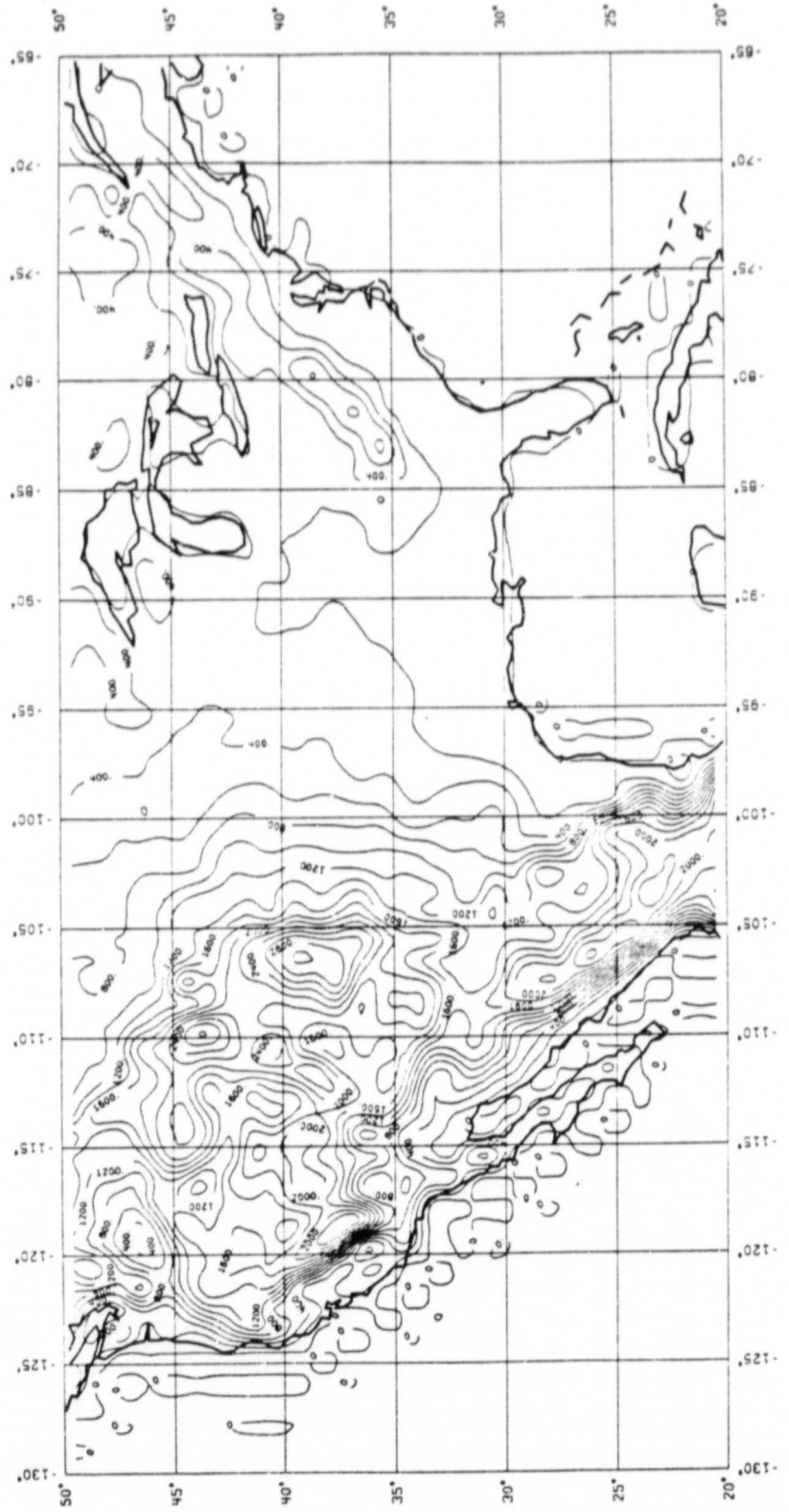

Figure 12: The contour map of the topographic heights above the geoid. This map was produced from 1°x1° mean elevations. The masses between the topographic surface and the geoid have to be condensed onto the geoid in the second method of Helmert's condensation. The contour interval of the map is 200 meters.

3.6(a), It was anticipated that the topographic masses further away from the computation point would have a very small contribution on the total potential change and thus the indirect effect. To test how the remote topographic masses have an influence on the indirect effect, cap sizes of 3°, 5° and 10° were used to compute the indirect effects at the center of each 1°x1° block in the test area and compared with those when the 20° cap was used. It was found that the differences are in the order of few tenths of a millimeter. The indirect effect computed using the masses only in the central 1°x1° block (called the 0° cap) were also used in the comparison. The maximum discrepancy was only 4 millimeters. The statistics of the indirect effects in the test area for the cap sizes of 0°, 5° and 20° are shown in Table 10. We can see that the remote topographic masses have insignificant contributions on the indirect effect due to the potential change at the centimeter level of accuracy. The insignificant contributions of the remote masses are understandable by examining the V_2 term of equation (86). The V_2 term consists of the factor $(\frac{hi}{\ell_{0i}})^3$. If the mean elevation of the block next to the central block is 1000 meters, then $\frac{h_j}{\ell_{0j}}$ of this block is less than 10^{-2} . By neglecting the mass of this block, the relative error in computing the indirect effect is less than 10^{-6} . Presumably, masses in the block further away from the central block cause a smaller relative error. As a result, the accumulation of relative errors in neglecting all masses around the central block is still very small and the effect of these masses is insignificant. From this investigation, we can say that only the mean elevation of the central block (block containing the computation point) is needed for computing the indirect effect due to the potential change.

To illustrate the indirect effect in the test area, the mean value at the center of each 1°x1° block was used to produce a contour map. The contour map of the indirect effects is shown in Figure 13. The maximum absolute value of the indirect effect in the test area is 51 cm. It occurs at the highest point in the area. We can observe the high correlation between the topography and the indirect effects by comparing Figure 12 and Figure 13. We see that the peaks of the indirect effects occur at the same locations where the peaks of topography occur. We can see also that the indirect effects due to potential changes in the ocean area are zero.

Table 10: The indirect effects ($\delta V/\gamma$) in the test area using different cap sizes (20°, 5° and 0° for the calculation of the potential changes.

Statistics	Capsize		
	20°	5°	0°
mean (m)	-0.0343	-0.0342	-0.0340
S.D (m)	0.0728	0.0728	0.0721
max (m)	0.0000	0.0000	0.0000
min (m)	-0.5076	-0.5076	-0.5036
RMS (m)	0.0805	0.0805	0.0798

4.2 Attraction Changes and Their Effects on Geoid Undulation

The attraction change due to the second method of Helmert's condensation for 1°x1° block was computed by the procedure explained in Section 3.6(b). In order to study the effects of remote masses on the attraction changes, cap sizes of 10° and 5° were used in the computation and compared with those when the 20° cap was used. Rapp's postulated model No. 1 for estimating the attraction change of the irregular part of the topography or the terrain correction was used in this study. Comparison of the three cap sizes is shown by the statistics in Table 11. The values under column "Difference between cap sizes" were obtained by subtracting the attraction change computed using one cap size from the other of the same 1°x1° block, then the statistics of the differences in the area were computed. From the table, we see the maximum absolute value of the difference from the 20° cap is 0.24 for the 10° cap and 0.69 for the 5° cap. Based on the most accurate values for the attraction changes that we obtain from the 20° cap, the root mean squares (RMS) of the differences of the 10° cap and 5° cap indicate no significant difference. In the mountainous terrain we have the larger magnitude of difference between the different cap sizes than that in the flat area. We must decide what order of magnitude differences can be tolerated in our work. In this study, the 10° cap was used for further investigation.

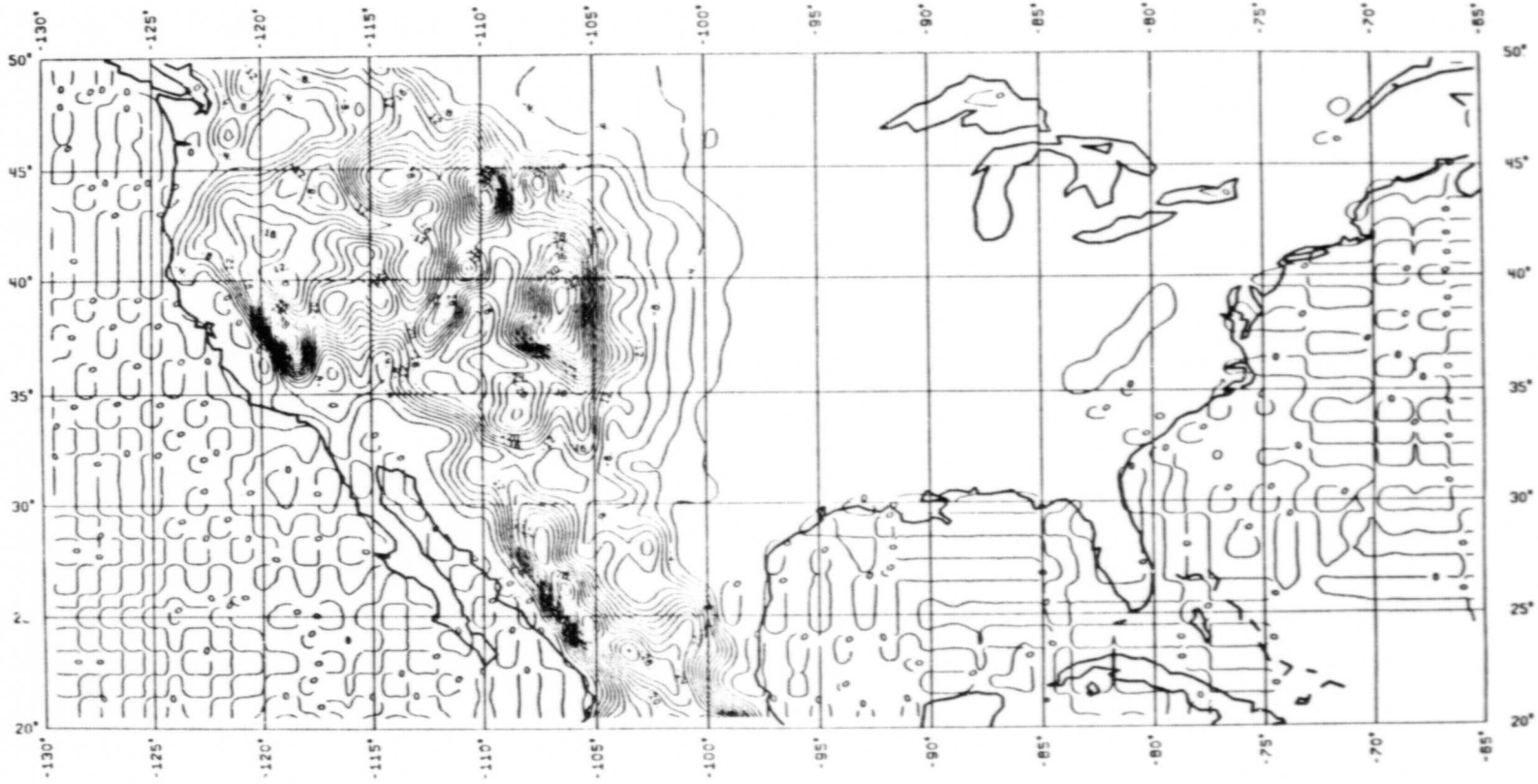

Figure 13: The contour map of the indirect effects due to the potential changes in the second method of Helmert's condensation. The potential change δV was computed at the center of each $1° \times 1°$ block using $1° \times 1°$ mean elevation with 10° cap. After the indirect effects had been calculated from $\delta N = \delta V/\gamma$, these values were used to produce the contour map. The contour interval of the map is 2 centimeters.

Table 11: Comparison of the attraction changes in the test area using different cap sizes (20°, 10° and 5°) for the computation.

Statistics	Cap Sizes			Difference between cap sizes	
	20°	10°	5°	20° and 10°	20° and 5°
mean (mgal)	2.1006	2.0848	2.0551	-0.0158	-0.0455
S.D. (mgal)	3.0510	3.0223	2.9685	0.0332	0.0964
max. (mgal)	11.7394	11.5009	11.0517	0.0000	0.0000
min. (mgal)	0.0013	-0.0025	-0.0047	-0.2386	-0.6877
RMS (mgal)	3.7036	3.6710	3.6098	0.0370	0.1067

Figure 14 is the contour map of the attraction changes in test area due to the Helmert's condensation method. This contour map was produced from 1°x1° grid values at the center of the blocks. Since the total attraction change is dominated by the terrain correction which is directly dependent on the elevation of the computation point, it can be anticipated that the peaks of the attraction changes occur where the peaks of the topography do. From this map, the areas having steep slopes are accentuated by the high gradients of the attraction changes. Similar to the potential change, there are no attraction change in the ocean area.

The attraction changes obtained from the previous step were used to compute the attraction change effect on geoid undulation. First we used Stokes' equation with cap size, σ_c of 10° (Method A in Section 3.3). There were two parts of the attraction change being computed, i.e., the effect of the regular part and the irregular part of the topography. Since the regular part has a small contribution on the total attraction change, we investigated how significant the attraction change of the regular part is in computing the correction to the geoid undulation. Two models of the attraction change were then used for this purpose. Model 1 consists of the attraction changes of both the regular and the irregular parts of the topography. Model 2 contains only the attraction change of the irregular

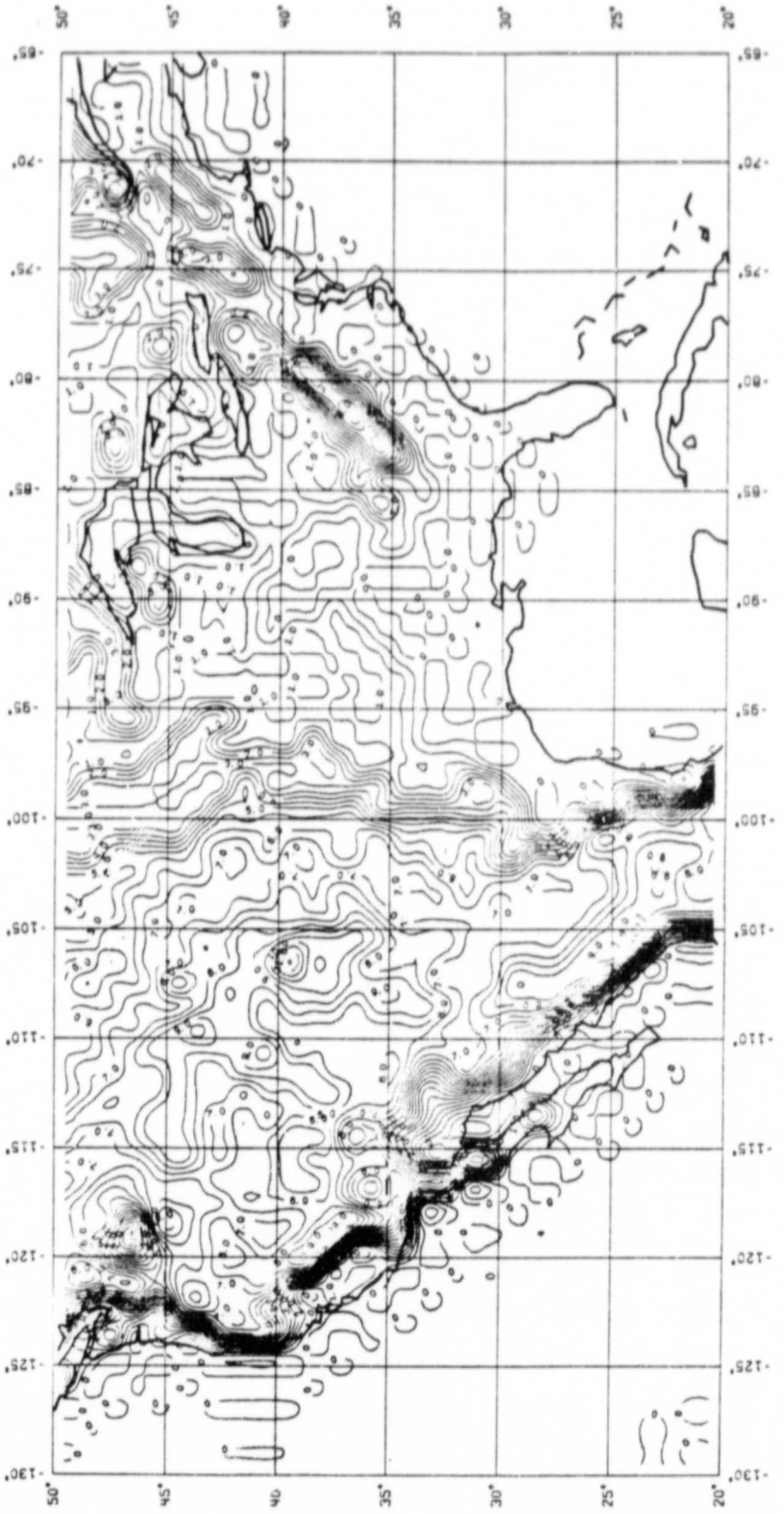

Figure 14: The contour map of the attraction changes due to the second method of Helmert's condensation. The attraction change was computed at the center of each 1°x1° block using Rapp's postualted model no. 1 (Table 9) and equations (65) and (66). These attraction changes were then used to produce the contour map. The contour interval of the map is 0.5 mgal.

part or the terrain correction. The result of using Stokes' equation (88) to compute the attraction change effect for geoid undulation is shown in Table 12. The maximum value in the area is 9.50 m computed by using model 1. Dimitrijevich et al. (1976) use an average value of the terrain correction over some defined cap to compute its effect on height anomalies. Their result for the 10° cap is the following:

Aver. terrain correction (mgal)	1	2	3	4	5	6	7	8	9	10	12	15
Height anomaly (m)	1.3	2.7	4.0	5.4	6.7	8.1	9.4	10.8	12.1	13.4	16.1	20.2

Considering this and the attraction changes shown in Figure 14, the maximum value of 9.50 m we have is not an unexpected magnitude which can be obtained for the 10° cap.

Table 12: Comparison of the attraction change effects on geoid undulation computed by using different models of the attraction change in the Stokes' equation (Method A) with $\sigma_c = 10°$.

Statistics	Corrections to geoid undulation due to attraction change (Method A equation (88))		Difference between Models
	Model 1	Model 2	A1 & A2
Mean (m)	2.7523	2.8361	0.0838
S.D. (m)	2.7887	2.8938	0.1077
Max. (m)	9.4970	9.9111	0.4318
Min. (m)	0.0000	0.0000	0.0000
RMS (m)	3.9176	4.0513	0.1365

A1 in Table 12 refers to the procedure whose attraction change effects on geoid undulation are computed by using model 1 of the attraction change in method A. If we take the difference between the undulation changes computed by method A using model 1 and model 2, and compute the statistics, we obtain the values in column "Difference between models A1 and A2." It can be seen

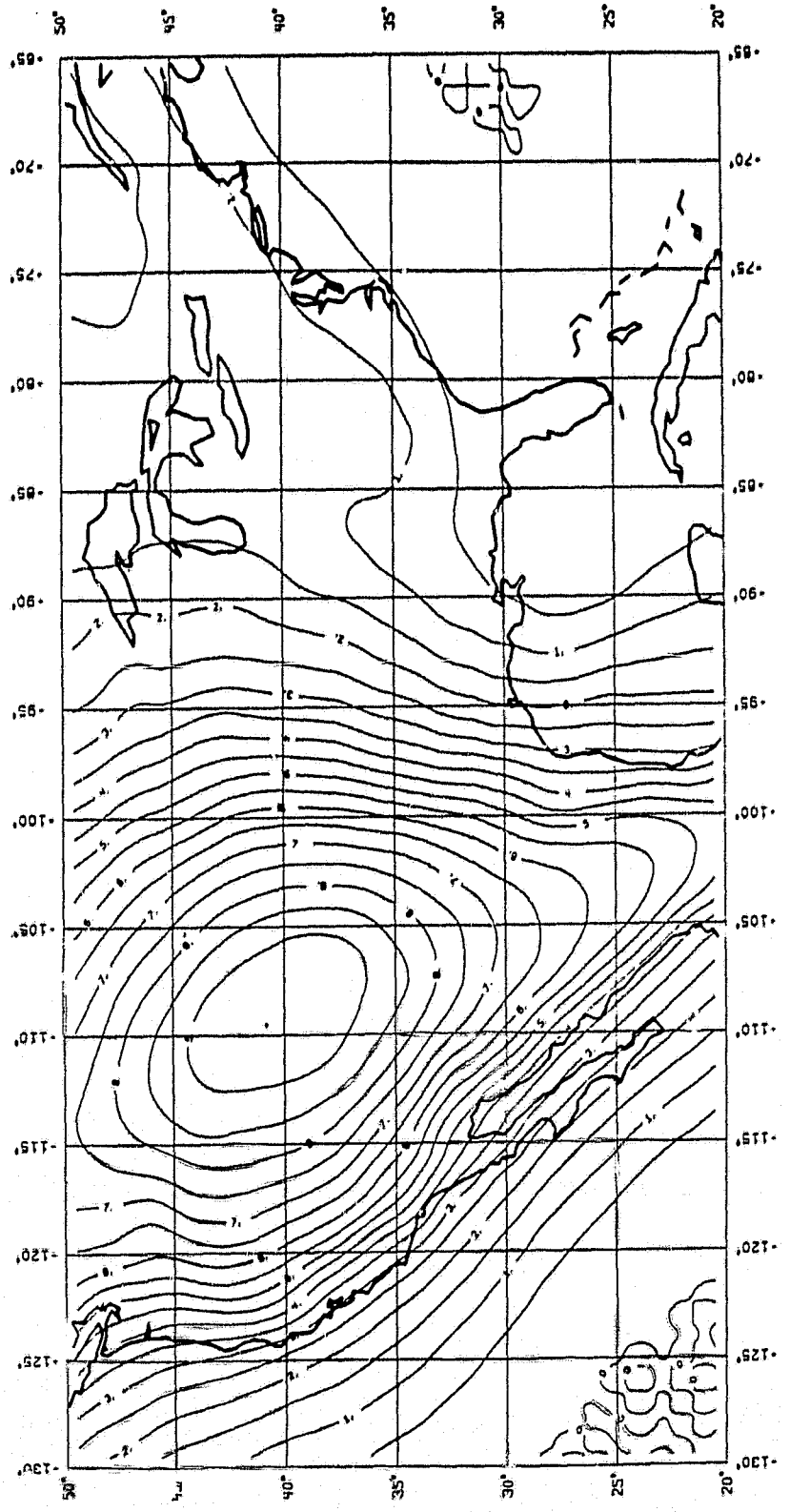

Figure 15: The contour map showing the attraction change effects on geoid undulation. The attraction change effect was computed at the center of each 1°x1° block using the attraction changes of both the regular and irregular parts of the topography (model 1) in the Stokes' equation (88) with $\sigma_C = 10°$. The 1°x1° grid values of the attraction change effects were then used to produce the contour map. The contour interval of the map is 0.5 meters.

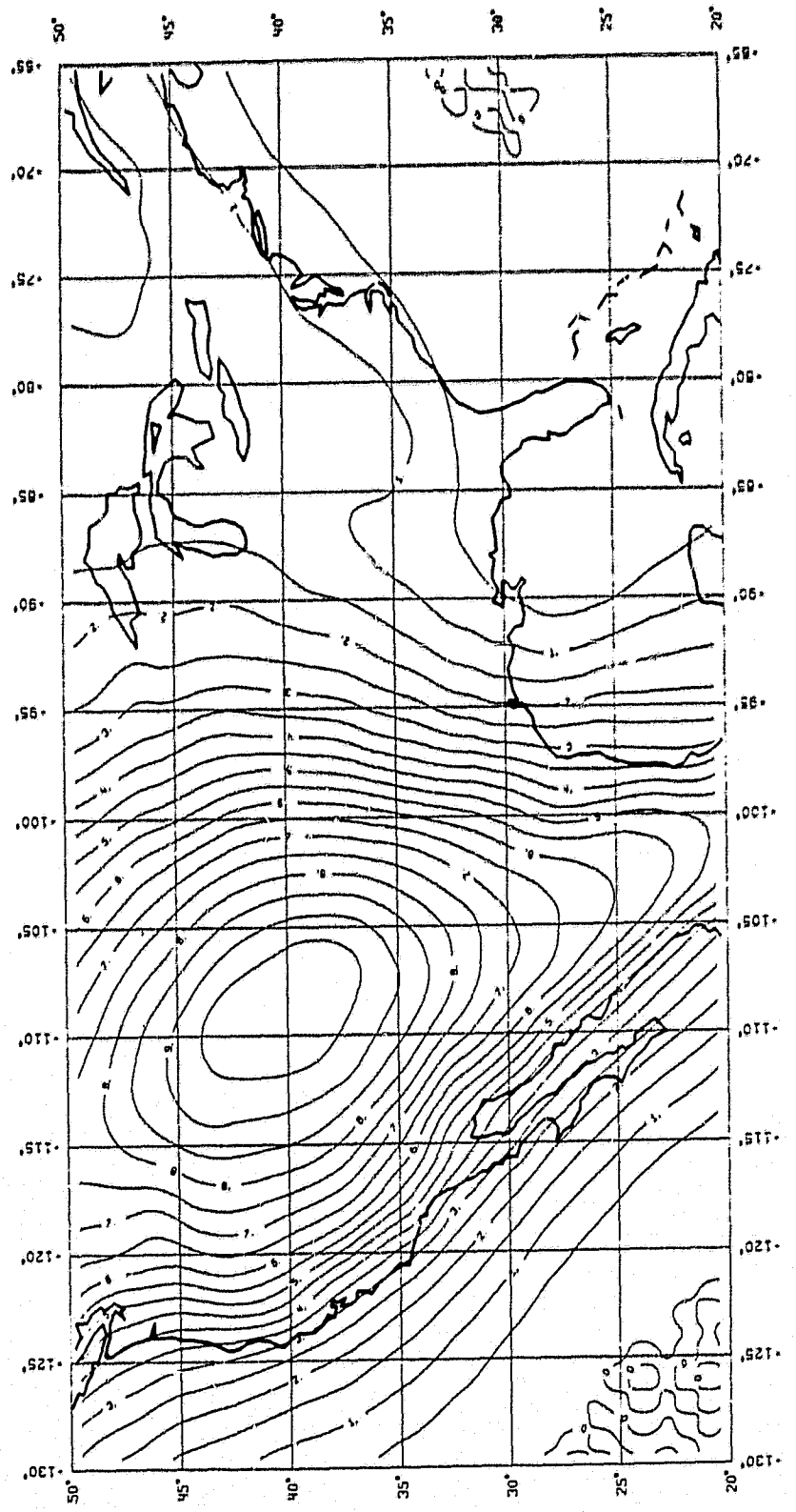

Figure 16: The contour map showing the attraction change effects on geoid undulation. The attraction change effect was computed at the center of each 1°x1° block using only the attraction change of the irregular part of the topography (model 2) in the Stokes' equation (88) with $\sigma_C = 10°$. The 1°x1° grid values of the attraction change effects were then used to produce the contour map. The contour interval of the map is 0.5 meters.

that RMS of the differences is 13.6 cm when we use model 2 instead of the more accurate model 1. Therefore, model 2 cannot be used as an approximation of attraction changes to compute the attraction change effects on geoid undulation for the geoid of 10 cm accuracy level. The contour maps of the corrections to the geoid undulation due to the attraction changes computed by Stokes' equation (88) using models 1 and 2 are shown in Figures 15 and 16 respectively. Comparing these two figures, we can see the major difference only in the highest contour of 9.5 m. The other contours are almost the same. We can see that the effect of the big mass in the high mountain area on the corrections to the geoid undulation can extend over the ocean area even if there are no attraction changes in the ocean area.

The 1°x 1° attraction over the whole world, were also used to develop a set of spherical harmonic coefficients. The set of spherical harmonic coefficients was developed into potential coefficients and anomaly coefficients (if $n < 2$) up to degree 180 (Colombo, 1981). These coefficients were then used to compute the corrections to the geoid undulations in the test area using equation (89). The correction computed by method B is shown in Table 13.

Table 13: Comparison of the corrections in gravity reduction computed from the harmonic coefficients (method B) with $\sigma_c = 10°$ and comparison between method A (see Table 12) and method B.

Statistics	ΔN by method B			Differences of ΔN between methods	
	Model 1	Model 2	Difference	A1 & B1	A2 & B2
Mean (m)	2.5469	2.9987	0.4519	-0.2055	0.1626
S.D. (m)	3.1513	2.9440	0.3881	0.5230	0.2944
Max. (m)	9.8689	10.1256	1.8309	0.6204	0.7758
Min. (m)	-1.9339	-0.1768	0.0934	-1.9339	-0.5501
RMS (m)	4.0512	4.2018	0.6001	0.5617	0.3363

The contour map of the attraction change effects on geoid undulation, produced from 1°x 1° grid values which were computed by method B via the spherical harmonic series (equation (89)) using model 1, is shown in Figure 17. Comparing Figure 17 to Figure 15, the patterns of the contours are the same. There are some contours extending over the ocean area on the east side of the continent.

Also shown in Table 13 are the differences of the corrections to geoid undulation due to the attraction change computed by methods A and B when the same model of the attraction change was used. Figure 18 is the contour map showing the differences of the corrections when model 1 of the attraction change was used. The differences between the two methods are systematic. The differences are caused by omitting the harmonic coefficients of degrees higher than 180. It was found that after the 1°x 1° attraction changes were transformed into the set of spherical harmonic coefficients (potential coefficients and anomalies coefficients (if $n < 2$)) up to degree 180, the attraction field was already distorted. The distortion of the field was detected by recreating the attraction changes from the set of the harmonic coefficients and comparing with the original attraction changes. Table 14 is the comparison by statistics in the test area between the original and the recreated attraction changes of model 1. The RMS difference is 0.6 mgal and the maximum difference is almost 3 mgal which is quite a large value.

Table 14: Comparison of the original attraction changes (model 1) and the recreated ones computed from the set of the spherical harmonic coefficients up to degree 180, (potential and anomaly coefficients (if $n < 2$)).

Statistics	Original Attraction changes	Recreated Attraction changes	Differences
Mean (mgal)	2.0975	1.9481	-0.1493
S.D. (mgal)	3.0353	3.1801	0.5951
Max. (mgal)	11.5884	10.4839	2.0466
Min. (mgal)	-0.0017	-1.6459	-2.8877
RMS (mgal)	3.6888	3.7287	0.6134

We furthered investigated how well equation (89) agrees with the Stokes' equation (88). The recreated attraction changes were therefore used to compute the corrections to the undulations due to the attraction changes by equation (88). The results were then compared with the corrections computed by equation (89). The statistics of the comparison in the test area is shown in Table 15. The mean difference is only 4.5 cm. This shows a good agreement of equation (89) and the Stokes' equation (88).

Table 15: Comparison of the attraction change effects on geoid undulation using equation (89) and the Stokes' equation with the recreated attraction changes from the harmonic coefficients.

Statistics	ΔN by Stokes' Eq. (88) with the recreated attraction changes	ΔN by harmonic series (equation (89))	Differences
Mean (m)	2.5922	2.5469	0.0453
S.D. (m)	3.1330	3.1513	0.1418
Max. (m)	9.8583	9.8689	0.4943
Min. (m)	-1.8844	-1.9339	-0.4797
RMS (m)	4.0657	4.0512	0.1488

4.3 Secondary Indirect Effect

From section 4.1 we have seen that the maximum and the mean indirect effects on geoid undulation, δN in the test area are 0.51 and 0.03 meters respectively. If we use equation (5) to compute the secondary indirect effect on gravity δ, we will have the maximum effect of only 0.15 mgal and the mean of 0.01 mgal. The magnitude of attractions in this order does not give any significant effect on the value of geoid undulation at all. Therefore, the computation of the secondary indirect effects on geoid undulation was neglected.

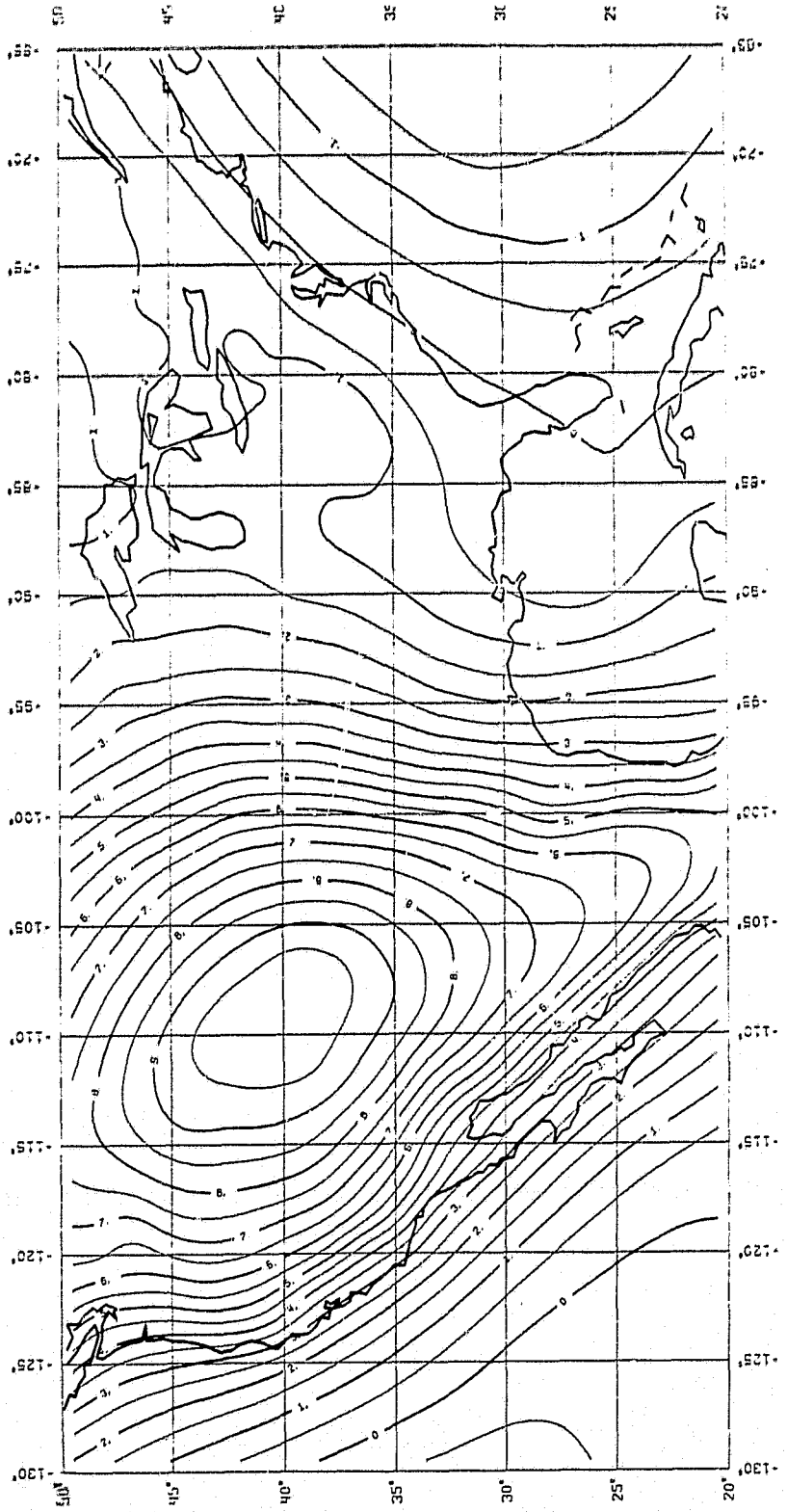

Figure 17: The contour map showing the attraction change effects on geoid undulation. The attraction change effect was computed at each center of 1°x1° block using the attraction changes of both the regular and irregular parts of the topography (model 1) in the spherical harmonic series (equation 89) with the 10° cap. The 1°x1° grid values of the attraction change effects were then used to produce the contour map. The contour interval of the map is 0.5 meters.

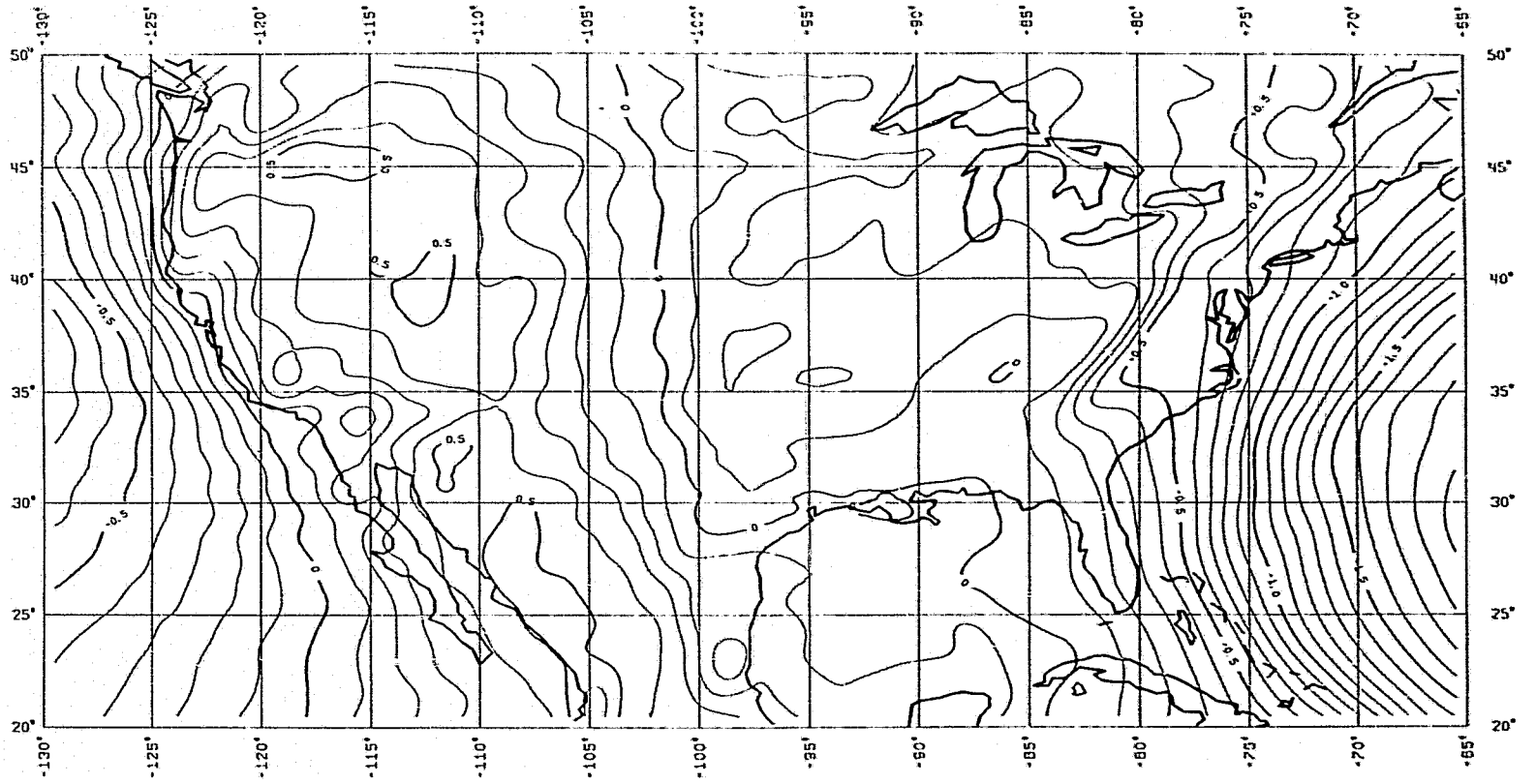

Figure 18: The contour map showing the differences of the attraction change effects on geoid undulation computed by method A (equation (88)) and method B (equation (89)). Model 1 of the attraction change was used in computing the attraction change effect. The contour map was produced from 1°x 1° grid values. The contour interval of the map is 0.1 meters.

4.4 Comparisons between Doppler and Topographically Corrected Gravimetric Undulations

The calculations derived in the previous sections represent theoretical concepts that should be subject to some actual verification. One way to do this is to compare geoid undulations implied by Doppler satellite observations at selected sites with those gravimetrically computed undulations based on data with and without the correction described in this study. A computation of the undulations, without correction terms, has been described by Lachapelle (1979) at 65 stations in the US using the GEM10B potential coefficients and mean surface gravity anomalies (uncorrected for terrain effect) of varying sizes of anomaly blocks i.e., 5'x5' , 30'x30' and 1°x1° blocks. These undulations are referred to as uncorrected gravimetric undulations.

Using the procedures of this paper, the correction terms were evaluated at each of the 65 stations. The correction terms applied to the station are the mean values of the block where the station is located. The attraction change corrections were computed using the direct integration procedure (equation (88)) and the spherical harmonic technique (equation (89)) based on 1°x1° mean attraction changes (the same values obtained in Section 4.2). By using 1°x1° attraction changes for computing the corrections, an inconsistency in the computation is created due to the fact that Lachapelle (ibid.) used 3 sizes of anomaly blocks. The inconsistency can be remedied if we were to use 5'x5' mean elevations to compute the attraction changes.

The corrections were used to compute a theoretically more correct undulation which is referred to as a topographic corrected gravimetric undulation. The corrected undulation was then compared with the Doppler derived undulation given by Lachapelle (ibid.). Before the actual comparisons are made, it is critical to make sure the Doppler undulations and the gravimetric undulations refer to the same ellipsoid.

In order to do this we first express the Lachapelle gravimetric undulations in the form:

$$N_{g,L} = \bar{N}_o + \bar{N}_g \qquad (91)$$

where $\bar{N}_o$ is the zero-order undulation of the geoid so that $N_{g,L}$ will refer to a specific ellipsoid. Values of $\bar{N}_g$ were computed by Lachapelle using constants of the Geodetic Reference System 1967 (GRS67). Lachapelle computed $\bar{N}_g$ and applied a correction of +25m (6378160-6378135m) to make the gravimetric undulations compatible with the ellipsoid used in the determination of Doppler undulations. Lachapelle then computed the mean difference ΔN defined as:

$$\Delta N = \frac{\sum_{i=1}^{n} \left[N_D - (\bar{N}_g + 25m)\right]}{n}$$

$$= \frac{\sum_{i=1}^{n} (N_D - \bar{N}_g)}{n} - 25m$$

where N_D is the Doppler derived undulation. Values of ΔN were determined using several sets of potential coefficients and anomaly sets. For our purpose we use the computations with the combination of GEM10B and the anomaly set. In this case the value of ΔN was -25.7 meters. Now Lachapelle gives the values of $\bar{N}'_g$ which are defined as:

$$\bar{N}'_g = \bar{N}_g + .25m + \Delta N$$

Thus we can re-construct the values of $\bar{N}g$ from the above equation:

$$\bar{N}_g = \bar{N}'_g - 25m - \Delta N \qquad (92)$$

Note that the mean values of $\bar{N}'_g$ would be zero with respect to the Doppler undulations.

In order to utilize these $\bar{N}_g$ values we must compute the zero-order undulation of the geoid so that undulation given by equation (91) will in fact refer to the Geodetic Reference System 1967. From Rummel and Rapp (1976, equation (25)) we have:

$$\bar{N}_o = \delta a\left[1 + \Phi(\psi_c)\right] - \frac{k\delta M}{\gamma R}\ \Phi(\psi_c)$$

where δa is the difference between the equatorial radius of the mean earth ellipsoid and that of GRS67, $k\delta M$ is the difference between the geocentric gravitational constant of the mean earth ellipsoid and that of GRS67, and $\Phi(\psi_c)$ is defined as:

$$\Phi(\psi_c) = \frac{1}{4\pi} \iint_{\sigma_c} S(\psi) d\sigma_c$$

Based on the recent estimates of the parameters of the mean earth ellipsoid, we find (see Appendix C)

$$\bar{N}_o = -26.11 \text{ meters}$$

Thus the geoid undulation with respect to GRS67 is the sum of $\bar{N}_o$ and $\bar{N}_g$ given by equation (92). Thus:

$$\bar{N}_{g,GRS67} = -26.11m - 25m + \bar{N}'_g - \Delta N$$

For comparisons with the Doppler undulations a correction of the above undulation is needed so that the values refer to the same ellipsoid. We would have

$$\bar{N}_{g,D} = \bar{N}_{g,GRS67} + (6378160 - 6378135m)$$

Thus

$$\begin{aligned} \bar{N}_{g,D} &= -26.11m - 25m + 25m + \bar{N}'_g - \Delta N \\ &= -26.11m + \bar{N}'_g - \Delta N \end{aligned}$$

For the ΔN of -25.7m we have

$$\bar{N}_{g,D} = \bar{N}'_g - 0.41 \text{ meters} \qquad (93)$$

We now are able to compare the values of $\bar{N}_{g,D}$ with the undulations derived from the Doppler stations. Such comparisons are given in the

first numerical column of Table 16. We see a systematic difference (Doppler minus gravimetric N) of 0.4 meters with a difference standard deviation of ±2.2 meters. At this point we apply the correction terms based on the Helmert's condensation procedure to the uncorrected (for topography) undulation given by equation (93). The details of the corrections at the 65 US stations are shown in Appendix B. The results of the comparisons are given in the last two columns of Table 16.

Table 16: The differences: Doppler undulation minus gravimetric undulations. The Doppler undulations are those from Lachapelle (1979).

Statistics of the Differences	Uncorrected Undulations Derived from Lachapelle (1979)	Corrected Undulations	
		When ΔN Computed by Equation (88)	When ΔN Computed by Equation (89)
Mean (m)	0.41	-3.42	-3.36
S.D. (m)	2.22	3.12	3.25
Max. (m)	5.83	5.03	5.23
Min. (m)	-3.78	-8.91	-9.29
RMS (m)	2.24	4.61	4.66

From Table 16, we can see the deterioration in the agreement between the gravimetric undulations and the Doppler undulations in all aspects, after the corrections were added. The absolute mean differences, the difference standard deviations and the difference RMS of the corrected sets are larger than the corresponding values of the uncorrected set.

In performing these comparisons we have assumed that the Doppler derived coordinates are geocentric since the gravimetrically determined values should theoretically be so. In fact there is a good evidence that there is a 4m z-axis shift of the Doppler origin with respect to the geocenter. Thus we should correct the original Doppler undulations to convert them to a true geocentric systems. We have:

$$N_D' = N_D + \Delta z \sin\phi$$

where Δz is the z-axis shift of the Doppler origin with respect to the geocenter, and ϕ is the geodetic latitude of the Doppler station. We now repeat our gravimetric-Doppler comparisons using the N_D' values. The results are given in Table 17.

Comparing Table 17 to Table 16, we see the decrease in the values of the difference standard deviations in all three sets of the gravimetric undulations. This indicates that the systematic effect due to z-shift of the Doppler origin with respect to the geocenter does exist.

Table 17: The differences: Doppler undulations minus gravimetric undulations. The Doppler undulations are those from Lachapelle (1979) corrected for systematic effect due to 4m z-axis shift.

Statistics of the Differences	Uncorrected Undulations Derived from Lachapelle (1979)	Corrected Undulations	
		When ΔN Computed by Equation (88)	When ΔN Computed by Equation (89)
Mean (m)	2.86	-0.97	-0.91
S.D. (m)	1.99	2.87	3.02
Max. (m)	7.87	6.78	6.98
Min. (m)	-0.90	-6.09	-6.63
RMS (m)	3.48	3.01	3.13

When the absolute mean differences of the corrected undulations are compared to that of the uncorrected undulations in Table 17, the improvement due to the topographic corrections is obvious. The standard deviations of the two corrected sets are however larger than that of the uncorrected set. The poorer standard deviations may be caused by the inaccurate values of the terrain corrections used in the computation of the attraction change effect on geoid undulation.

5. Summary and Conclusion

The indirect effects on the geoid computation due to the second method of Helmert's condensation were studied. Theoretically, the use of Helmert's

anomalies in Stokes' equation should give a more accurate geoid than the use of uncorrected free-air anomalies. Using Helmert's anomalies gives three types of corrections to the free-air geoid. First, the indirect effects on the geoid undulation are the result of the potential changes in condensing the topographic masses above the geoid onto the geoid in Helmert's reduction method. The second one is the correction to geoid undulation affected by the attraction changes in the reduction process. The third one is the secondary indirect effects on geoid undulation which is the consequence of the indirect effects caused by the potential changes.

The computation or evaluation point for computing a potential change in a gravity reduction is not at the same location as the computation point for computing an attraction change. In the second method of Helmert's condensation, the potential change is the difference between the potential of the topography and the potential of the condensed layer, evaluated at some point P_0 on the geoid. The attraction change, on the other hand, is the difference between the vertical attraction of the topography and the vertical attraction of the condensed layer. It is evaluated at a point P on the earth's surface.

In the derivation of potential changes and attraction changes, the topographic masses above the geoid are divided into a "regular" part and an "irregular" part (Moritz, 1968). The "regular" part of the topography is sometimes regarded as an approximation to the actual topography. Three models can be used to represent the regular part of topography: the spherical Bouguer plate, the plane circular plate and the infinite plane plate. The "irregular" part of the topography consists of the topographic masses which deviate from the plate surface.

The first part of this investigation was an investigation of the potential change and the attraction change of the regular part of topography as computed from the three different models. These changes were then compared with the irregular part when the same amount of mass was used. We found the closest agreement between the results from the plane circular plate and the irregular part of the topography.

Next we developed computation techniques to compute the potential changes and the attraction changes from 1°x 1° mean elevations. A test area covering the United States was then used to investigate the actual effects of the three corrections to the free-air geoid. It was found that the maximum indirect effect on geoid undulation (potential change effect) in the test area was 51 centimeters. The maximum attraction change effect on geoid undulation was 9.50 meters when the 10° cap was used in Stokes' equation (88). The attraction change effect on geoid undulation computed from the set of harmonic coefficients (equation (89)) up to degree 180 was not the same as that computed by Stokes' equation. The discrepancy between the two methods was mainly caused by the higher degree coefficients being omitted. We have shown that equation (89) produced results approximately equal to Stokes' equation (88) when the same attraction change field was used in both equations.

The secondary indirect effects on gravity were of small magnitudes in the test area, the mean value in the area being 0.01 mgal. Thus, the effects could be neglected in the computation.

Doppler and gravimetric undulations reported by Lachapelle (1979) were used to investigate how well the corrections due to the potential changes and attraction changes could improve the gravimetric undulations. The gravimetric undulations were slightly modified so that they would be comparable to the Doppler derived undulations, i.e., they would refer to the same ellipsoid (section 4.4). These undulations are referred to as the uncorrected gravimetric undulations. The corrections were then applied to the uncorrected undulations to obtain the so called topographically corrected gravimetric undulations.

Since there is a tendency that the Doppler origin may have a z-axis shift of 4 meters with respect to the geocenter. The corrections due to this shift were computed and applied to Lachapelle's Doppler undulations to get the "corrected" Doppler undulations. The uncorrected and the corrected gravimetric undulations were then compared with the original and the corrected Doppler undulations.

Our comparisons confirm that there exists the z-shift in the Doppler origin. Based on this fact, the corrections due to the potential changes and the attraction changes in the Helmert's condensation, show that systematic differences are reduced although the dispersion of the results increases. More specific conclusions depend on the determination of more accurate terrain correction values.

The terrain correction used in this study directly depended on the elevation of the evaluation point. The type of terrain surrounding the evaluation point was not considered. This assumption leads to a remarkable error in the terrain correction when the evaluation point is located on a high plateau. In such an area, the terrain correction would be very small, or zero, if equation (87) were used. Accurate values for the terrain correction may be obtained if mean elevations in smaller blocks were used as done in Dimitrijevich et al. (1976) (5'x 5' blocks) and Curiale et al. (1981) (5/8'x 5/8' blocks).

If the more accurate corrections due to the attraction change still cannot improve the agreement of the Doppler undulations and the corrected gravimetric undulations, it is suspected that Helmert's anomalies may not be appropriate for geoid computation in the high mountain area such as the Rocky Mountains.

It is recommended, then, that the use of Molodensky's correction in mountainous regions be studied to see if a better agreement between gravimetric and Doppler undulations may result. Two comments should be made in regards to solving the Molodensky boundary value problem. One is that instead of the geoid undulation, the height anomaly is obtained from the solution. It is stated by Heiskanen and Moritz (1967, p. 294) that these two are very close in magnitude. The second point is that the linear dependency of the gravity anomaly on the elevation must not be presumed. The reason for this is that the assumption will lead us to the first-order correction (G_1 term) which is the same as the terrain correction (Moritz, 1980, p. 414).

REFERENCES

Baeschlin, C.F., Textbook of Geodesy, Technical Translation, Aeron. Chart & Information Centre, St. Louis, 1948.

Bomford, G., Geodesy, Oxford University Press, 1971.

Colombo, O., Numerical Methods for Harmonic Analysis on the Sphere, Dept. of Geodetic Science, Report No. 310, The Ohio State University, Columbus, 1981.

Curiale, J.S., C.T. Ford, P.D. Martzen, and G.E. Roberts, Gravity Reduction Analysis (status report), Geodynamics Corporation, August 1981.

Dimitrijevich, I.J., "The Use of Terrain Corrections in Computing Gravimetric Deflection of Vertical Componenets and Geoid Heights", DMAAC, St. Louis, Missouri, April 1972.

Dimitrijevich, I., J.J. G'Schwind, and J.A. Treiber, "Gravimetric Parameters (Zeta, Xi, Eta) for the Redondo Peak Region of New Mexico, as Calculated from Terrain Corrected Gravity Anomalies", DMAAC, St. Louis, Missouri, April 1976.

Forsberg R. and C. Tscherning, "The Use of Height Data in Gravity Field Approximation by Collocation", Journal of Geophys. Res., Vol. 86, No. B9, pp. 7843-7854, Sept. 10, 1981.

Fryer, J.G., The Effect of the Geoid on the Australian Geodetic Network, Unisurv Report No. 20, Univ. of New South Wales, Kensington, N.S.W., 1970.

Grushinsky, N.P., The Theory of the Figure of the Earth, 1963, Translated from Russian, 1969.

Heiskanen, W. and H. Moritz, Physical Geodesy, W.H. Freeman and Co., San Francisco, 1967.

Lachapelle, G., "Comparison of Doppler-Derived and Gravimetric Geoid Undulations in North America", Proceedings of Int'l. Geodetic Symposium on Satellite Doppler Positioning, Austin, Texas, January 1979.

Lambert, W.D., "The Reduction of Observed Values of Gravity to Sea Level", Bull. Geod., No. 26, pp. 107-181, 1930.

Lambert, W. and F. Darling, Tables for Determing the Form of the Geoid and Its Indirect Effect on Gravity, U.S. Coast and Geodetic Survey, Spec. Publ. No. 199, 1936.

MacMillan, W.D., The Theory of the Potential, Dover Publications, New York, 1958.

Mather, R.S., The Non-Regularised Geoid and Its Relation to the Telluroid and Regularised Geoids, Unisurv Report No. 11, Univ. of New South Wales, Kensington N.S.W., 1970.

Moritz, H., Linear Solutions of the Geodetic Boundary-Value Problem, Dept. of Geodetic Science, Report No. 79, The Ohio State University, Columbus, December 1966.

Moritz, H., On the Use of Terrain Correction in Solving Molodensky's Problem, Dept. of Geodetic Science, Report No. 108, The Ohio State University, Columbus, May 1968.

Moritz, H., Fundamental Geodetic Constants, the Report of SSG5.39 of IAG, XVII General Assembly of IUGG, Canberra, 1979.

Moritz, H., Advance Physical Geodesy, Abacus Press, Tunbridge Wells, Kent, U.K., 1980.

Neequaye, B.A., Helmert's Condensation Method of Gravity Reduction, A Technical Essay, Department of Geodetic Science, The Ohio State University, Columbus, Ohio, Winter Quarter 1975.

Rapp, R.H., "Determination of Potential Coefficients to Degree 52 from 5 Degree Mean Gravity Anomalies", Bull. Geod. No. 51, pp. 301-323, 1977.

Rapp, R.H., Ellipsoidal Corrections for Geoid Undulations Computations, Dept. of Geodetic Science, Report No. 308, The Ohio State University, Columbus, March 1981.

Rapp, R.H., A Summary of the Results from the OSU Analysis of Seasat Altimeter Data, Dept. of Geodetic Science and Surveying, Report No. 335, The Ohio State University, Columbus, August 1982.

Rapp, R.H., and R. Rummel, Methods for the Computation of Detailed Geoids and their Accuracy, Dept. of Geodetic Science, Report No. 233, The Ohio State University, Columbus, 1975.

Rummel, R., and R. Rapp, "The Influence of the Atmosphere on Geoid and Potential Coefficient Determinations from Gravity Data", Journal of Geophys. Res., Vol. 81, No. 32, pp. 5649-5653, Nov. 10, 1976.

Appendix A
Derivation of Equation (89)

Two methods for computing the geoid undulation are presented in section 3.1. The undulations computed by both methods must be the same. If we equate equations (74) and (77), we get

$$\frac{R}{4\pi\gamma}\iint_{\sigma_c}(\Delta g_I - \Delta g_{ref})\,S(\psi)\,d\sigma_c + R\sum_{n=2}^{\bar{n}} A_n = \frac{R}{4\pi\gamma}\iint_{\sigma_c}\Delta g_I\,S(\psi)\,d\sigma_c + \frac{R}{2\gamma}\sum_{n=2}^{\infty} Q_n\,\Delta g_n \qquad (A1)$$

where

$$A_n = \sum_{m=0}^{n}(\bar{C}^*_{nm}\cos m\lambda + \bar{S}_{nm}\sin m\lambda)\,\bar{P}_{nm}(\sin\bar{\phi})$$

$$\Delta g_n = \gamma(n-1)\,A_n$$

The maximum degree $\bar{n}$ of the harmonic series is usually selected in such a way that the error in neglecting the higher degree terms ($n > \bar{n}$) will be very small. The upper limit of the summation in the second term on the right hand side of equation (A1) then can be set to $\bar{n}$. The lower limit of this summation must be extended to zero because the zeroth- and the first-degree components of Δg do exist in the set of the harmonic coefficients developed from the attraction changes. Since the zeroth and the first-degree potential coefficients are not defined, we have to use the anomaly coefficients to compute the components Δg_0 and Δg_1. Equation (A1) can be written as:

$$\frac{R}{4\pi\gamma}\iint_{\sigma_c}(\Delta g_I - \Delta g_{ref})\,S(\psi)\,d\sigma_c + R\sum_{n=2}^{\bar{n}} A_n = \frac{R}{4\pi\gamma}\iint_{\sigma_c}\Delta g_I\,S(\psi)\,d\sigma_c + \frac{R}{2\gamma}\sum_{n=0}^{\bar{n}} Q_n\,\Delta g_n$$

$$\frac{R}{4\pi\gamma}\iint_{\sigma_c}\Delta g_{ref}\,S(\psi)\,d\sigma_c = R\sum_{n=2}^{\bar{n}} A_n + \frac{R}{2\gamma}\sum_{n=2}^{\bar{n}} Q_n\,[\gamma(n-1)\,A_n] + \frac{R}{2\gamma}\sum_{n=0}^{1} Q_n\,\Delta g_n = \frac{R}{2}\sum_{n=2}^{\bar{n}}(2 - Q_n(n-1))\,A_n + \frac{R}{2\gamma}\sum_{n=0}^{1} Q_n\,\Delta g_n \qquad (A2)$$

C-2

If $\bar{C}_{nm}^{(\Delta g)}$ and $\bar{S}_{nm}^{(\Delta g)}$ are anomaly coefficients, then we can compute g_n by:

$$\Delta g_n = \sum_{m=0}^{n} (\bar{C}_{nm}^{(\Delta g)} \cos m\lambda + \bar{S}_{nm}^{(\Delta g)} \sin m\lambda) \bar{P}_{nm}(\sin\Phi)$$

Thus equation (A2) can be used to compute the undulation from harmonic coefficients within the cap size of σ_c when the zeroth and the first-degree components of Δg exist.

To transform equation (A2) to equation (89), the following list is used:

Equation (A2)	Equation (89)
Δg	δA
A_n	δA_n
Δg_n	$\delta \overline{A}_n$
$\bar{C}^*_{nm}$, $\bar{S}_{nm}$	δC_{nm} , δS_{nm}
$\bar{C}_{nm}^{(\Delta g)}$, $\bar{S}_{nm}^{(\Delta g)}$	$\delta C_{nm}^{(\Delta g)}$, $\delta S_{nm}^{(\Delta g)}$

Appendix B

Comparison between Doppler and Topographic Corrected Gravimetric Undulations

Notations used in the table:

N_D = doppler derived undulations (from Lachapelle, 1979)

$\bar{N}_g$ = uncorrected gravimetric undulations (see Section 4.4)

$DN = N_D - \bar{N}_g$

δN = correction due to the potential change

ΔN^1 = correction due to the attraction changes computed by Stokes' equation (88)

$\bar{N}g^1$ = the corrected gravimetric undulation when ΔN^1 is used
$= \bar{N}g + \delta N + \Delta N^1$

$DN^1 = N_D - \bar{N}g^1$

ΔN^2 = correction due to the attraction changes computed by the harmonic series (equation (89))

$\bar{N}g^2 = \bar{N}g + \delta N + \Delta N^2$

$DN^2 = N_D - \bar{N}g^2$

Point Number	Latitude	Longitude	N_D	$\bar{N}_g$ GEM10B +Δg	DN	δN	When ΔN was Computed by eq. (88)			When ΔN was Computed by eq. (89)		
							ΔN^1	$\bar{N}^1_g$	DN^1	ΔN^2	$\bar{N}^2_g$	DN^2
60001	39 1 39.8	283 10 27.7	-34.63	-32.08	-2.55	0.00	1.02	-31.06	-3.57	0.41	-31.67	-2.96
51003	38 12 7.3	282 37 35.4	-34.87	-32.12	-2.75	0.00	1.02	-31.10	-3.77	0.30	-31.82	-3.05
51008	34 2 10.8	281 50 40.3	-39.18	-37.75	-1.43	0.00	0.62	-37.13	-2.05	0.11	-37.64	-1.54
51012	30 39 5.8	274 11 38.3	-28.74	-31.40	2.66	0.00	0.32	-31.08	2.34	0.30	-31.10	2.36
51025	30 54 24.7	266 23 56.4	-28.54	-30.56	2.02	0.00	1.44	-29.12	0.58	1.44	-29.12	0.58
51039	30 52 15.4	258 3 58.9	-24.55	-27.94	3.39	-0.03	6.02	-21.95	-2.60	6.11	-21.86	-2.69
51048	34 56 43.5	253 32 24.0	-20.40	-23.83	3.43	-0.18	8.46	-15.55	-4.85	8.72	-15.29	-5.11
51052	32 43 24.9	248 29 5.6	-32.52	-33.88	1.36	-0.03	6.24	-27.67	-4.85	6.77	-27.14	-5.38
51062	32 32 36.2	242 57 35.7	-35.93	-39.93	4.00	0.00	3.20	-36.73	0.80	3.38	-36.55	0.62
52063	36 54 50.8	239 26 45.2	-34.18	-36.84	2.66	-0.61	3.66	-33.19	-0.99	3.81	-33.04	-1.14
51065	35 25 28.9	243 6 48.5	-31.44	-33.67	2.23	-0.03	6.37	-27.33	-4.11	6.17	-27.53	-3.91
51067	32 57 45.0	261 54 35.8	-28.53	-31.46	2.93	-0.01	4.48	-26.99	-1.54	4.37	-27.10	-1.43
51068	30 41 46.3	278 15 59.8	-29.15	-31.30	2.15	0.00	0.32	-30.98	1.83	0.08	-31.22	2.07
51069	32 45 31.7	279 26 37.4	-33.52	-33.79	0.27	0.00	0.48	-33.31	-0.21	0.14	-33.65	0.13
51094	41 18 46.2	285 59 38.2	-34.08	-31.36	-2.72	-0.01	1.21	-30.16	-3.92	0.50	-30.87	-3.21
51095	43 13 24.3	289 18 28.8	-27.46	-25.88	-1.58	0.00	1.08	-24.80	-2.66	0.21	-25.66	-1.80
51103	32 4 19.5	253 31 4.4	-24.82	-28.49	3.67	-0.13	7.73	-20.86	-3.96	8.07	-20.52	-4.30
51118	42 37 21.7	288 30 42.4	-29.44	-27.42	-2.02	0.00	1.04	-26.20	-3.24	0.17	-27.25	-2.19
51121	30 37 55.2	267 59 3.1	-28.24	-30.21	1.97	0.00	1.12	-29.09	0.85	1.12	-29.09	0.85
51122	37 2 23.1	282 58 43.8	-35.48	-33.70	-1.78	0.00	0.88	-32.82	-2.66	0.30	-33.40	-2.08
51123	30 40 16.4	255 58 37.1	-20.57	-26.40	5.83	-0.09	6.93	-19.56	-1.01	7.27	-19.22	-1.35
51124	31 2 7.2	259 55 8.4	-23.09	-26.19	3.10	-0.02	5.75	-20.46	-2.63	5.74	-20.47	-2.62
51126	30 31 37.0	276 12 32.2	-28.52	-30.48	1.96	0.60	0.33	-30.15	1.63	0.21	-30.27	1.75
51153	30 17 19.6	262 44 58.6	-26.51	-29.91	3.40	0.00	3.58	-26.33	-0.18	3.49	-26.42	-0.09
51161	34 7 23.4	245 19 25.8	-31.98	-34.59	2.61	-0.01	6.20	-28.40	-3.58	6.36	-28.24	-3.74
51186	37 48 21.6	237 32 45.8	-33.98	-35.09	1.11	0.00	2.92	-32.17	-1.81	2.87	-32.22	-1.76
51188	34 12 16.9	241 49 44.4	-34.93	-37.99	3.06	-0.03	4.12	-33.90	-1.03	4.25	-33.77	-1.16
51189	34 45 59.6	242 10 49.7	-33.97	-36.42	2.45	-0.05	4.80	-31.67	-2.30	4.92	-31.55	-2.42
51920	35 11 48.2	245 57 32.6	-29.08	-31.05	1.97	-0.04	6.80	-24.29	-4.79	7.11	-23.97	-5.11
30078	42 37 4.3	288 30 32.5	-29.37	-27.41	-1.96	-0.01	1.04	-26.38	-2.99	0.17	-27.25	-2.12
51015	25 53 26.2	279 41 35.0	-26.36	-31.43	5.07	0.00	0.04	-31.39	5.03	-0.16	-31.59	5.23
51014	27 57 25.3	279 26 32.6	-29.43	-32.64	3.21	0.00	0.14	-32.50	3.07	-0.11	-32.75	3.32
51009	33 7 3.4	273 39 1.5	-30.77	-30.29	-0.48	0.00	0.69	-29.60	-1.17	0.63	-29.66	-1.11
52030	35 47 1.4	262 1 11.7	-28.62	-28.05	-0.57	-0.01	4.17	-23.88	-4.74	4.00	-24.05	-4.57
51033	41 42 12.6	264 21 20.1	-29.14	-28.53	-0.61	-0.01	3.56	-25.07	-4.07	3.31	-25.32	-3.82
51041	41 38 26.7	258 24 2.0	-20.05	-20.20	0.15	-0.06	7.02	-13.24	-6.81	7.15	-13.11	-6.94
51043	44 48 1.4	251 39 17.0	-13.04	-13.58	0.54	-0.12	8.88	-4.82	-8.22	9.03	-4.67	-8.37
51044	41 36 55.7	252 12 54.5	-15.17	-15.41	0.24	-0.27	9.26	-6.42	-8.75	9.80	-5.88	-9.29
51054	37 23 19.4	250 53 14.0	-21.04	-22.91	1.87	-0.19	9.13	-13.97	-7.07	9.54	-13.50	-7.48
51056	40 38 36.1	248 1 43.2	-17.80	-18.81	1.01	-0.24	9.22	-9.83	-7.97	9.74	-9.31	-8.49
51057	40 23 41.7	244 47 31.6	-20.20	-20.60	0.40	-0.21	8.02	-12.79	-7.41	8.51	-12.30	-7.90
51058	39 49 37.6	241 0 53.0	-25.72	-25.43	-0.29	-0.11	6.46	-19.08	-6.64	6.85	-18.69	-7.03
52066	44 23 31.2	238 42 12.9	-22.24	-21.27	-0.97	-0.07	5.28	-15.97	-6.27	5.76	-15.58	-6.66
52074	42 7 21.4	238 10 22.4	-23.11	-23.71	0.60	-0.12	5.45	-18.38	-4.73	5.76	-18.07	-5.04
52075	46 55 8.3	246 57 3.3	-13.94	-13.54	-0.40	-0.18	8.28	-5.44	-8.50	8.69	-5.03	-8.91
52076	48 11 54.9	256 2 29.4	-18.26	-16.43	-1.83	-0.03	5.79	-10.67	-7.59	5.80	-10.66	-7.60
52077	48 4 38.5	260 6 48.0	-22.84	-20.44	-2.40	-0.01	4.20	-16.25	-6.59	4.07	-16.38	-6.46
53078	46 6 5.1	263 27 56.6	-29.20	-25.42	-3.78	-0.01	3.48	-21.95	-7.25	3.28	-22.15	-7.05
52079	43 53 0.7	264 4 15.1	-27.18	-25.54	-1.64	-0.01	3.57	-21.98	-5.20	3.35	-22.20	-4.98
51082	43 44 11.1	275 11 32.8	-33.62	-33.50	-0.12	0.00	1.33	-32.17	-1.45	1.11	-32.39	-1.23
51089	38 8 31.7	238 16 34.2	-34.65	-34.42	-0.23	0.00	3.95	-30.47	-4.18	4.09	-30.61	-4.04
52093	47 40 33.0	243 41 21.1	-17.53	-17.37	-0.16	-0.06	7.40	-10.01	-7.52	7.72	-9.69	-7.84
51104	47 47 7.4	251 22 4.9	-15.66	-14.28	-1.38	-0.05	7.58	-6.75	-8.91	7.77	-6.56	-9.10
51106	46 23 30.5	272 1 11.4	-36.38	-33.57	-2.81	-0.01	1.47	-32.11	-4.27	1.18	-32.40	-3.98
52119	46 15 32.1	267 5 0.6	-28.76	-26.70	-2.06	-0.01	2.40	-24.31	-4.45	2.10	-24.61	-4.15
51127	47 11 6.5	240 39 43.9	-21.41	-20.71	-0.70	-0.02	6.42	-14.31	-7.10	6.55	-14.18	-7.23
51144	39 13 26.6	261 27 28.1	-26.36	-26.23	-0.13	-0.02	5.30	-20.95	-5.41	5.12	-21.13	-5.23
51166	40 14 7.0	274 10 27.1	-35.29	-34.02	-1.27	0.00	1.29	-32.73	-2.56	1.13	-32.89	-2.40
51167	31 12 37.7	270 16 30.6	-28.09	-29.13	1.04	0.00	0.61	-28.52	0.43	0.59	-28.54	0.45
51168	37 33 6.9	273 55 10.4	-32.67	-32.26	-0.41	0.00	1.03	-31.23	-1.44	0.95	-31.31	-1.36
51170	33 28 42.7	268 59 50.9	-27.16	-27.94	0.78	0.00	1.26	-26.68	-0.48	1.16	-26.78	-0.38
51174	40 49 20.3	270 42 40.2	-35.00	-32.04	-2.96	0.00	1.67	-30.37	-4.63	1.47	-30.57	-4.43
51175	41 48 20.4	267 33 2.7	-33.50	-31.89	-1.61	0.00	2.42	-29.47	-4.03	2.24	-29.65	-3.85
51176	40 5 10.6	278 15 39.9	-36.30	-33.24	-3.06	-0.01	1.25	-32.00	-4.30	1.01	-32.24	-4.06
51179	39 44 44.1	237 50 53.7	-30.45	-30.43	-0.02	-0.02	3.58	-26.57	-3.88	3.90	-26.55	-3.90

Appendix C
The Zero Order Undulation

The zero order undulation for the geoid computation by Method 1 and 2 of section 3.1 is given by (Rummel and Rapp, 1976, equation (25)):

$$\bar{N}_o = \delta a \left[1 + \Phi(\psi_c)\right] - \frac{K\delta M}{\gamma R}\Phi(\psi_c) \qquad (C1)$$

with

$$\Phi(\psi_c) = \frac{1}{4\pi}\iint_{\sigma_c} S(\psi)\,d\sigma_c \qquad (C2)$$

where δa is the difference between the equatorial radius of the mean earth ellipsoid and that of the adopted reference ellipsoid, and $k\delta M$ is the difference between the geocentric gravitational constant of the mean earth ellipsoid and that of the adopted ellipsoid.

Note that $\bar{N}_o$ in equation (C1) is not that as N_o given in equation (75). This is because the global mean anomaly, Δg_o must be subtracted from Δg_I in the second term of equations (74) and (78), to assure that the gravity anomalies used in Stokes' equation have a global average equal to zero. See the detailed derivation in Rummel and Rapp (ibid).

At the present, the best-known constants for the mean earth ellipsoid which will be used in our calculations are:

(from Moritz, 1979),

$kM = 3.9860047 \times 10^{14}\ m^3/sec^2$

(from Rapp, 1982),

$a = 6378135.6$ m.

The constants for the Geodetic Reference System 1967 (GRS67) are:

$kM = 3.98603 \times 10^{14}\ m^3/sec^2$

$a = 6378160$ m.

That is $k\delta M = -253 \times 10^7\ m^3/sec^2$ and $\delta a = -24.4$ meters.

For a cap of 10° in Stokes' integral, $\Phi(\psi_c = 10°) = 0.2068$. Using R = 6371000 meters and $\gamma = 9.8$ m/sec^2, the zero order undulation of GRS67 is:

$N_o = -26.11$ meters.